TECHNICAL MEMORANDUM

401

The ECMWF Re-Analysis of the Mesoscale Alpine Programme Special Observing Period

Christian Keil and Carla Cardinali

Research Department

March 2003

European Centre for Medium-Range Weather Forecasts
Europäisches Zentrum für mittelfristige Wettervorhersage
Centre européen pour les prévisions météorologiques à moyen terme

For additional copies please contact

The Library
ECMWF
Shinfield Park
Reading
RG2 9AX
library@ecmwf.int

Series: ECMWF Technical Memoranda

A full list of ECMWF Publications can be found on our web site under:
http://www.ecmwf.int/publications/

Abstract

At ECMWF, a reanalysis of the 70-day Special Observing Period (SOP) of the Mesoscale Alpine Programme (MAP) in autumn 1999 has been produced using the global assimilation system 4D-Var with a horizontal resolution of approximately 40 km (T511/159L60). Additional MAP observations used in the MAP reanalysis comprise e.g. European windprofilers, high-resolution radiosondes and surface observations. Four of the 16 European windprofilers reporting during the SOP had to be denied in the reanalysis due to their variable quality. The assimilation of the MAP observations leads to moister conditions in the southern Alpine region, southern France and over the Adriatic Sea while drier conditions prevail along the Alpine mountain chain. A data impact study shows that the windprofilers introduce changes in the divergent wind field which feeds back on the humidity analysis and slightly dries the troposphere in the southern Alpine region. The investigation on some IOPs illustrates some specific aspects of the MAP Re-Analysis. Finally, a comparison of GPS derived integrated water vapour contents and the analyzed counterparts shows that the analyzed humidity field well describes the inter-diurnal humidity variations at southern Alpine GPS stations. However, the analyses seem to be slightly too dry compared with GPS measurements.

1 Introduction

In meteorology, an analysis represents an image of the true state of the atmosphere at a given time. Analyses not only provide initial conditions for numerical weather forecasts but they can be used as a comprehensive diagnostic of the atmosphere or to check the quality of new observations.

The Mesoscale Alpine Programme (MAP) Special Observing Period (SOP) took place from 7 September to 15 November 1999 and involved a large number of additional upper-air soundings and instrumented flights, along with an exceptional concentration of surface measurements (Bougeault et al., 2001). The use of the ECMWF 12-hour 4D-Var global assimilation system in conjunction with MAP observations provides a new, more accurate reference of the atmosphere at high resolution and with dense in-situ measurements in the Alpine region.

The objectives of the MAP Re-Analysis are to:

- produce a comprehensive set of analyses describing the state of the atmosphere for the 70-day period of MAP SOP in autumn 1999.
- Create a formatted archive of the additional MAP observations.
- Foster European and international research by making the observations and the analyses archive widely available.
- Perform validation and diagnostic studies.
- Indicate the benefit of the use of additional observations through data impact studies.

This report can be divided in two main parts: sections 2-5 provide a general description of the performance of the MAP Re-Analysis, while in sections 6 and 7 the quality of the MAP Re-Analysis is investigated for different Intensive Observation Periods (IOP). Aspects of the ECMWF Integrated Forecasting System (IFS) are provided in section 2 followed by an overview of the characteristics of MAP observations and their usage (section 3). A quality assessment of these additional observations is presented in section 4 before the general impact of the MAP-suite and the MAP observations is discussed in section 5. Case-study-type investigations of some IOPs in section 6 are complemented by an evaluation of the analyzed humidity field using GPS derived integrated water vapour measurements (section 7). After concluding remarks in section 8, the appendix contains more

details of the quality of the European windprofilers, an overview of the MAP Re-Analysis products as well as the MARS retrieval template.

2 The Model System

Over the last years, a considerable improvement in the accuracy of forecasts from global numerical weather prediction (NWP) systems has been achieved. Since autumn 1999, when the MAP field experiment took place, there have been substantial modifications in the IFS (Simmons and Hollingsworth, 2002). The main model changes between the operational IFS in 1999 (cycle 21R2; denoted OPER'99 henceforth) and the version used for the MAP Re-Analysis (cycle 24R3; denoted MAP-suite henceforth) are briefly summarized.

During the SOP on 12 Oct 1999, the number of vertical levels increased from 50 to 60, a new orography and associated subgrid orographic fields were introduced, and changes occurred in the cloud and convection schemes (Gregory et al., 2000). In 2000, other major changes involved an increase of the horizontal resolution from approximately 60 to 40 km (T319 to T511 spherical-harmonic representation), a revised treatment of the land surface scheme and a new parameterization of the long wave radiation. In the assimilation system, the 6-hour window 4D-Var has been extended to 12-hour (Bouttier, 2001a) and the inner-loop resolution increased from T63 to T159 (approximately 120 km horizontal resolution). Recently, a new shortwave radiation transfer model and new bias correction for satellite observations were included in the IFS.

On the data usage, the improved version of RTTOV fast radiative transfer model (Matricardi et al., 2001) has facilitated a better use of satellite data in the MAP-suite, also neither SSM/I wind information nor brightness temperatures from the HIRS instrument were used in OPER'99 (see Tab. 1). Introduced in July 1999, dropsondes (Cardinali, 1999) and American windprofiler data (Bouttier, 2001b) have been used in OPER'99. Moreover, the increased analysis resolution allowed more use of aircraft data in the MAP-suite (Cardinali et al., 2003). Globally, these changes in the use of observations mainly affect the satellite sounding data (SATEM) resulting in an increase of more than 300 % while aircraft data use increases about 40 % in the MAP-suite. The additional MAP observations account for a global increase of about 35 % for PILOTs (including pilot balloons and windprofilers), 26 % and 23 % for radiosondes and SYNOP stations, respectively.

At the start of the MAP Re-Analysis Project at ECMWF, cycle 24R3 was created for the 12-hourly 4D-Var global assimilation system. This cycle became operational on 22 Jan 2002. Data of some satellite sounding instruments were available but not used in OPER'99, e.g. AMSU-A channel 14 which is sensitive in the stratopause region and ocean surface windspeed data from the SSM/I instrument. This data is used in the MAP Re-Analysis. With the new system version, some bias tuning was necessary to use 1999 satellite data.

Table 1: Difference in data usage between OPER'99 and the MAP-suite.

Observation type	Instrument	Used Parameters	OPER'99	MAP-suite
SYNOP	synop surface data	RH2m, PS	yes	yes & MAP-data
TEMP	radiosondes	u,v,T,q	yes	yes & MAP-data
	Europ. dropsonde	u,v,T	no	MAP-data
PILOT	Europ. profiler	u,v	no	MAP-data
AIREP	AMDAR etc.	u,v,T	yes	more & MAP-data
SATEM	TOVS AMSU-A	Tb	yes	more
	TOVS HIRS	Tb	no	yes
	SSM/I	windspeed	no	yes
	SSM/I	TCWV	yes	more

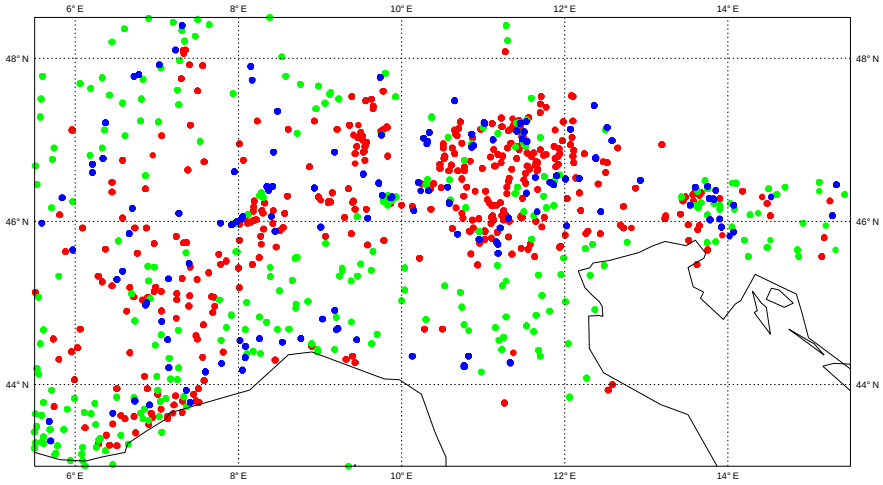

Figure 1: Location and colour-coded usage of the surface stations in the Alpine region: used (green), blacklisted due to 'peak'-effect (blue) and due to 'valley'-effect (red).

For instance, the mean bias of SSM/I total column water vapour (TCWV) used over oceans has been reduced to 0.79 kg/m^2, which is comparable to current operational values (OPER'99 shows larger bias amounting to 2.48 kg/m^2 for the same 5-day period in mid-September 99).

3 MAP observations

3.1 MAP Surface data

During the entire SOP, nearly 3 million observations of ∼10800 synoptic land stations have been archived. These surface stations were reporting pressure, temperature and humidity. However, only two observed values are assimilated: the relative humidity (RH2m) and the surface pressure (ps).

Additionally, in the IFS there is another constraint on the usage of observations from synoptic land stations. If the station height is differing by more than 200 m from the corresponding model orography representation, the observations recorded at these synoptic stations are not representative and consequently discarded. In the MAP-suite, this prescribed threshold results in an exclusion of 40 % of all MAP surface stations, of which 28 % are declined because the model resolution is not resolving the Alpine valleys ('valley'-effect, i.e. model height - 200 m> station altitude) and the rest 12 % because the Alpine mountain peaks are higher than the model orography ('peak'-effect, i.e. model height + 200 m < station altitude; Fig. 1).

3.2 European windprofiler during MAP

European windprofiler data has only recently been incorporated in data assimilation schemes. Data quality was a significant issue before the data could be reliably used. Therefore, during the MAP-SOP no European windprofiler data distributed in real-time via GTS (Global Telecommunication System) were operationally assimilated in NWP models. At ECMWF, the monitoring of European windprofilers started in 2000 (Bouttier, 2001b and Andersson and Garcia-Mendez, 2002). The assimilation of European windprofilers started on 9 April 2002 in the operational model suite (cycle 25R1), using 8 out of the 17 windprofiler stations from which data has been received.

Table 2: Available European windprofilers during the MAP SOP. The four stations in brackets have been denied in the MAP Re-Analysis.

Station ID	Latitude	Longitude	Name	Country	Elevation [m]	Vertical Range
3501	52.42	-4.00	Aberystwyth	UK	50	TROP/LST
3807	50.13	-5.10	(Camborne)	UK	88	BL/TROP
3840	50.87	-3.23	(Dunkeswell)	UK	253	BL/TROP
6348	51.95	4.88	Cabauw	NL	0	BL
6792	46.47	9.72	Julier Pass	CH	2233	BL
7112	48.61	0.87	La Ferte Vidame	F	245	TROP/LST
7115	45.56	8.71	Lonate	I	146	TROP/LST
7613	45.56	8.71	Lonate	I	146	BL/TROP
7615	43.11	5.92	Toulon	F	7	BL/TROP
7626	43.12	0.37	Lannemezan	F	600	BL/TROP
7453	45.71	3.09	(Clermont)	F	660	BL/TROP
10394	52,21	14.13	Lindenberg	D	107	BL/TROP/LST
11105	47.18	9.36	Bad Ragaz	CH	435	BL
11036	48.10	16.60	Vienna	A	227	BL
11120	47.16	11.23	Innsbruck	A	593	TROP
16228	42.40	13.40	(L'Aquila)	I	1000	TROP

During the MAP SOP, 16 European windprofilers in 7 countries were active (Tab. 2). Altogether these stations reported 46620 atmospheric profiles of the wind components with different vertical and temporal resolution. The vertical range of the profilers differs from station to station depending on the frequency at which the radar instrument operates. Four of the 16 windprofilers detect the boundary layer (BL), 12 reach the mid-troposphere (TROP) and three profilers reach the lower stratosphere (LST). Many stations report twice hourly, while Aberystwyth reports every 8 minutes.

Consequently, a temporal as well as vertical thinning of the data has been applied according to operational procedures, *i.e.* the 12 hourly 4D-Var window has been divided in 30-minute time-slots, within which only one profile per station is used. These half-hourly time-slots match well the temporal reporting frequency of most European windprofilers. Vertically, the profiles have been thinned to one observation every 5 hPa (or 5 % of pressure above 100 hPa).

Since there has been no monitoring on the quality of European windprofilers available during the SOP, data of all stations has been used in a pilot analysis experiment. Having performed this analysis experiment for the first two weeks of the SOP, it became evident that data of some European windprofilers were deteriorating the quality of the analyses. Therefore, in the MAP Re-Analysis observations from four European windprofiler stations (Camborne, Dunkeswell, Clermont and L'Aquila) have been denied (see section B in appendix). Following current operational procedures, the observation error of windprofiler is equal to that of a radiosonde observation (see section 4).

3.3 High resolution radiosoundings

During the SOP, 5165 radiosonde measurements were flown from 20 European stations. Some were started at extra MAP radiosonde locations (e.g. Verona, Sterzing) while at numerous operational stations (e.g. Milano, Udine and Bologna) the radiosonde ascent frequency was increased (to 3 hourly). Some of the high resolution radiosondes were reporting data from more than 3000 levels per ascent. Since ECMWF's assimilation system technically can deal with only 300 levels per ascent, the soundings were linearly thinned. Using a simple

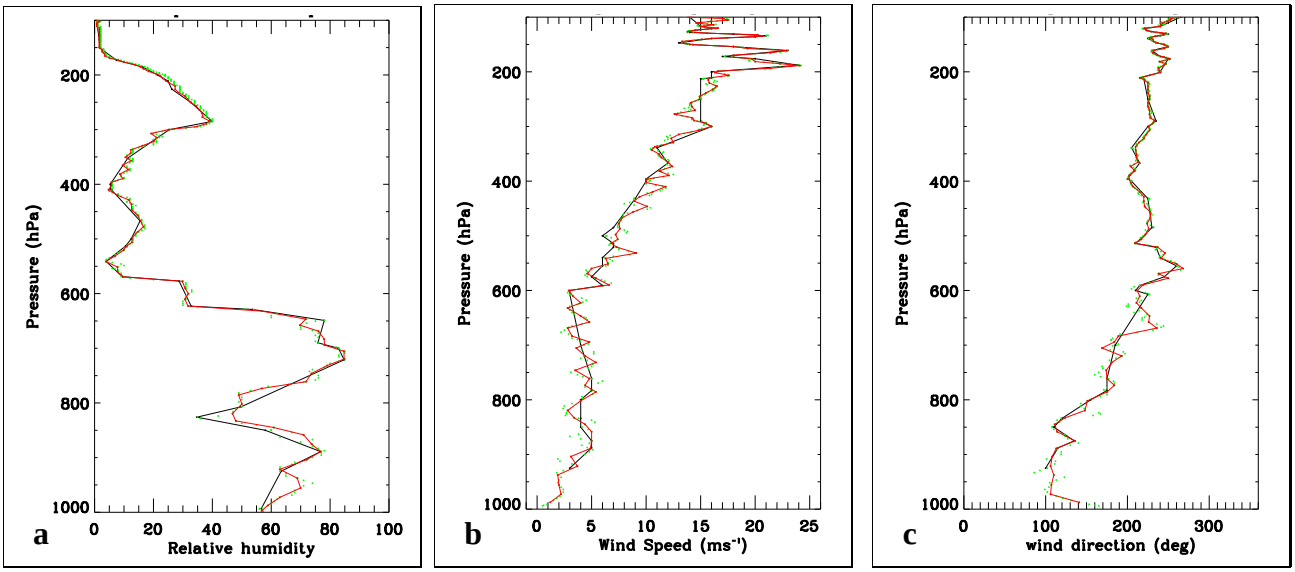

Figure 2: Comparison of GTS data (black), high resolution SOP profile (green) and thinned SOP profile (red) for (a) relative humidity, (b) wind velocity and (c) direction at Milano on 17 Sep 99 12 UTC.

thinning technique, evenly spaced data points have been selected from each high resolution profile.

The thinned profiles closely follow the high resolution data set and show more vertical variability than the one transmitted via GTS (thinned by Vaisala method, WMO), as can be seen for the Milano station on 17 Sep 99 12 UTC (Fig. 2). The GTS profile shows $\pm$ 10 % maximum error for the relative humidity (Fig. 2a; 950 and 800 hPa) and $\pm$ 2 m/s for wind (Fig. 2b) with respect to both the higher resolution profiles.

3.4 Aircraft data and dropsondes

The eight research aircrafts deployed during the IOPs reported data along their flight path with very high temporal resolution. The amount of data gathered by these research aircrafts is similar to the one reported by commercial aircrafts across the Alpine region. However, their contribution to the overall assimilated aircraft data in the MAP-suite is negligible (less than 1 %) due to thinning procedures. Likewise, the amount of used dropsondes which were released from the research aircrafts during IOPs amounts to less than 1 % compared with radiosonde data.

4 Assessment of the quality of MAP observations

Standard deviation (STD) and bias of observation departures from the background (12-hour forecast from a previous assimilation cycle) and from the analysis are useful as they provide information to validate the assimilation performance. In particular, the decrease of STD of analysis departure with respect to the background departure indicates to which extent the assimilation model was able to fit different observation types. Recent work on the improvement in skill of NWP (Simmons and Hollingsworth, 2002) has shown that the short-range forecast error (1-day) has been reduced to the order of magnitude of the observation error. Large observation departures from the background would be then a sign of poor quality of the observations.

Apart the MAP Re-Analysis (Exp-ID: e9mi; denoted MAP-RA henceforth, see Table 3), three other analysis experiments have been performed using the MAP-suite to assess the performance and the impact of MAP

Table 3: Overview of data usage in different analysis experiments using the MAP-suite: GTS denote data broadcast via the GTS, MDC the MAP observations provided by the MAP Data Centre (MDC).

Experiment-Name Experiment-ID Experiment period		ALDAT e9cp 7 -21 Sep	CNTRL e9ex 7 Sep-16 Nov	NOPRO e9jr 7 Sep-7 Oct	MAP-RA e9mi 7 Sep-16 Nov
Data type	Used Parameters				
synop surface data	RH2m, PS	GTS + MDC	GTS	GTS + MDC	GTS + MDC
radiosondes	u,v,T,q	GTS + MDC	GTS(6 h)	GTS + MDC	GTS + MDC
Europ. dropsonde	u,v,T	MDC	none	MDC	MDC
Europ. profiler	u,v	all 16 profilers	none	none	12 profilers
aircraft data	u,v,T	GTS + MDC	GTS	GTS + MDC	GTS + MDC

observations. First, since there has been no monitoring of European windprofiler data in 1999, a pilot analysis experiment using all additional MAP observations has been carried out for two weeks in Sep 99 (Exp-ID: e9cp; denoted ALDAT henceforth). Second, a control experiment has been performed excluding all MAP observations for the entire SOP (Exp-ID: e9ex; denoted CNTRL henceforth). Third, an analysis experiment without the European windprofiler data has been completed for the first 30 days of the SOP to investigate their role in more detail (Exp-ID: e9jr; denoted NOPRO henceforth).

The MAP-RA and CNTRL differ mainly in the usage of the MAP SOP observations. However, due to an error in the operational blacklist file, the American profilers were used in the control experiment in the whole troposphere, whereas in the MAP-RA only above 700 hPa (current corrected operational usage). Moreover, few dropsondes available next to tropical storms were neglected in CNTRL. During MAP, data of the increased ascent frequency at operational radiosonde stations (3 hourly) was transmitted via GTS and subsequently used in operational analysis. To exclude any additional MAP observations and replicate the routine ascent frequency of European radiosondes, only 6 hourly radiosonde data has been used in CNTRL.

For the first two weeks of the MAP SOP, the background and analysis departures STD of experiment ALDAT have been calculated and compared with respect to CNTRL. These comparisons give evidence that some of the extra observations are deteriorating the analysis quality. The STD of e.g. the U-component of the wind of the observation types TEMP (radiosondes) and PILOT (pilotsondes) are larger for ALDAT than for CNTRL (Fig. 3a,b). PILOT departures show significant differences in the mid-troposphere. The deterioration of the radiosonde fit could be due to the extra radiosondes assimilated but also to some other observation types that measure wind.

Apart from radio- and pilotsoundings, windprofilers are reporting information on the flow field at high temporal and vertical resolution. The standard deviation of the background departures of the European windprofilers peaks around $5\,m/s$ in the mid-troposphere (Fig. 3c) which is considerably larger than the values of radio- and pilotsoundings and well above the mean observation error ($3\,m/s$ in the mid-troposphere, Tab. A.1). Also, there are more windprofiler measurements in the mid-troposphere than there are radio- and pilotsondes. Thus, the magnitude of STD of the background departures of the European windprofilers as well as the fit degradation in ALDAT with respect to CNTRL for radio- and pilotsondes suggest that some profilers are poor.

In order to be able to identify the European windprofilers reporting poor quality measurements, observation statistics has been calculated individually for each station (see section B in appendix). Consequently, it has been decided to exclude four of the 16 European windprofilers in the MAP-RA, for which the bias is exceeding the predescribed observation error: Camborne (UK), Dunkeswell (UK), Clermont (F) and L'Aquila (I) (Fig. B.1 b,c,h and m). Omitting these four windprofilers results in a significant improvement: smaller standard deviation of background and analysis departures for the remaining European windprofilers (Fig. 4c) and

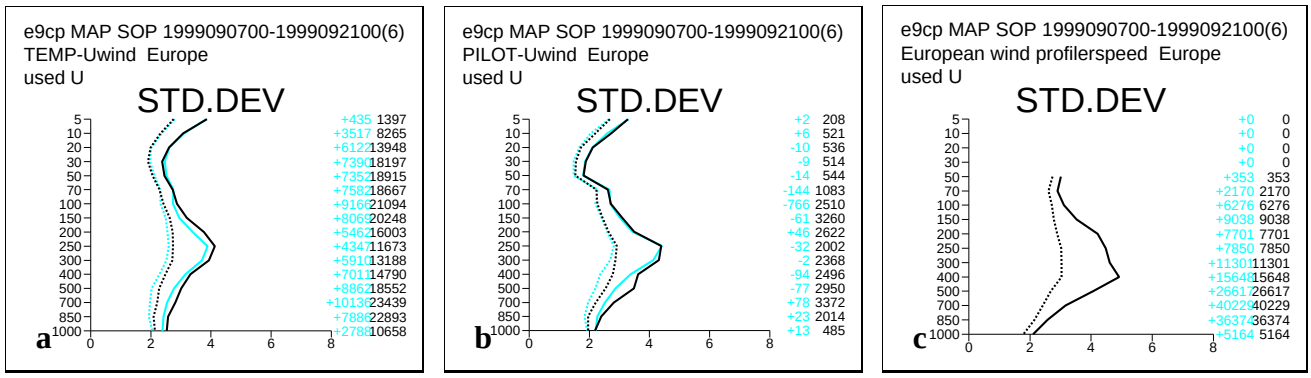

Figure 3: Two weeks standard deviation of the background (o-b; solid line) and analysis (o-a; dotted) departures of the U-component of the wind for the observation types TEMP (a), PILOT (b) and European windprofiler (c) for ALDAT. The reference experiment is CNTRL (blue). The numbers indicate the amount of data used with the difference (blue numbers) showing the excess of observations w.r.t. CNTRL.

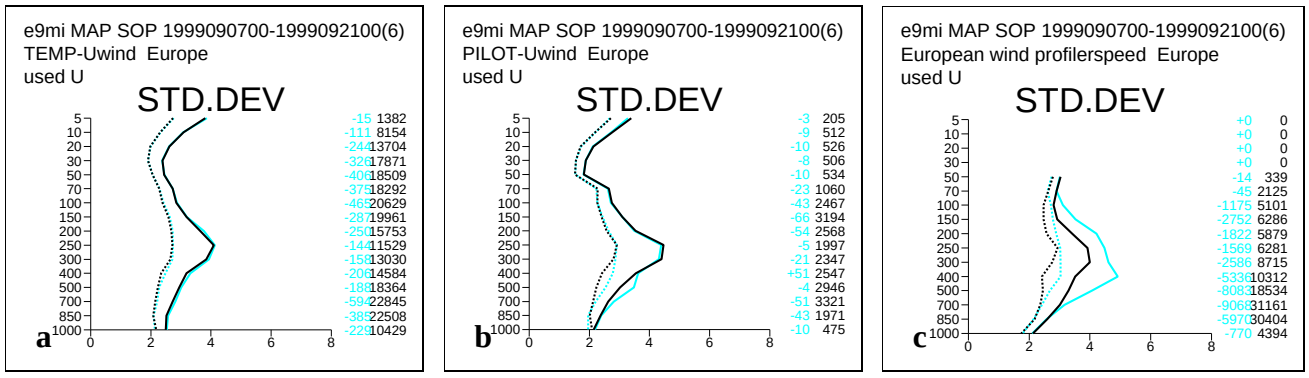

Figure 4: As Fig. 3 but for MAP-RA (black line). The reference experiment is ALDAT (blue). The numbers indicate the amount of data used with the difference (blue numbers) showing the excess of observations w.r.t. ALDAT.

reduced standard deviation with respect to ALDAT for TEMP and PILOT observations, Fig. 4a and b, respectively. The windprofiler standard deviation of the background departures is less than 4 m/s and comparable to the magnitude of the assigned observation error (Fig. 4c). The amount of windprofiler data used is reduced by 30 % compared to ALDAT.

Calculated for the full SOP, observation statistics for TEMPs and European windprofilers are similar, with the standard deviation of the background departures meandering around 3 m/s and peaking at 300 hPa at the jet stream level (Fig. 5). The bias of the departures of both observation types remains close to zero. Similarities in statistics between TEMPs and European windprofilers confirm the equal weight given in the assimilation process to both the observation types. The amount of used TEMPs is outnumbering the European windprofilers, with even more TEMPs contributing in the upper troposphere and lower stratosphere. In the MAP-RA, about 40 % of the available windprofiler data has been assimilated, with considerable differences in usage between the sites: 81 % of Lindenberg reports has been used, 74 % at Lonate and only 34 % at Aberystwyth (due to its very high reporting frequency).

Focussing on humidity observations, the additional MAP high resolution radiosondes increase the usage of TEMP humidity data in MAP-RA by a factor of 4 compared to CNTRL in the Alpine region (43-49 ° N and 2-17 ° E). Generally, the bias of background and analysis departures is small (less than 0.3 g/kg; not shown). In the boundary layer below 700 hPa, CNTRL shows a negative bias, *i.e.* CNTRL is slightly too moist with

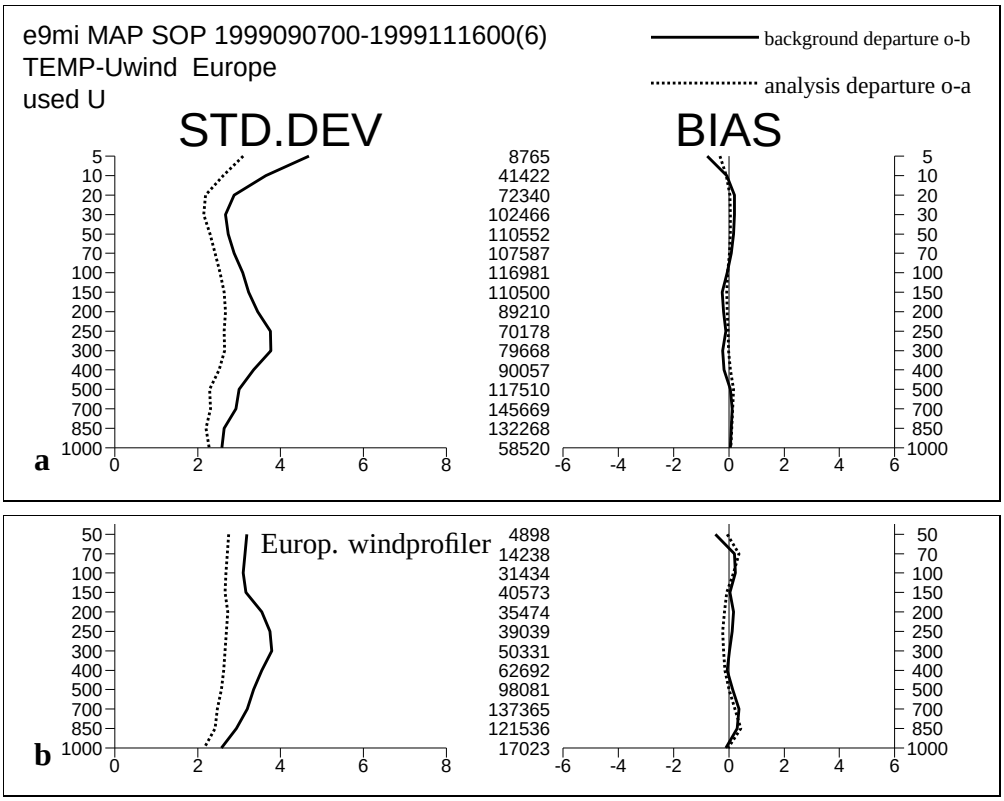

Figure 5: Standard deviation and bias of the background (o-b; solid line) and analysis (o-a; dotted) departures of (a) the U-component of the wind for the observation types TEMP and (b) European windprofiler of the MAP-RA for the entire SOP. The numbers indicate the amount of data used.

respect to observations. Above 700 hPa, the bias is close to zero showing a good agreement of CNTRL and radiosonde observations. For MAP-RA, the bias of background departure is about 0.1 g/kg higher than in CNTRL, resulting in less moist conditions below 700 hPa and slightly drier ones aloft. However, the bias of the analysis departure of MAP-RA is smallest throughout the troposphere, *i.e.* MAP-RA agrees better with observations than CNTRL (not shown).

Also, data of the additional MAP surface stations contribute to a large increase in the usage of humidity observations in the Alpine region (Tab. 4). These surface observations multiply the usage in MAP-RA by a factor of 5 (MAP-RA vs OPER'99), while the higher resolution of the MAP-suite accounts for an increase of only 15 % (CNTRL vs OPER'99). Both the higher horizontal resolution and the increased density of surface observations lead to a more efficient use of SYNOP RH2m measurements (30 % of all surface data have been used in MAP-RA, 25 % in CNTRL and 22 % in OPER'99). Still, the majority of surface data is rejected due to the mismatch of the station height and the corresponding model orography representation in mountainous regions.

Table 4: Some statistics on surface humidity observations used in different analyses for an Alpine domain bounded by 43-49 ° N and 2-17 ° E.

	total data	used data	background departure (o-b)		analysis departure (o-a)	
			mean [%]	RMS [%]	mean [%]	RMS [%]
OPER'99	398704	88574	4.02	12.0	2.01	8.95
CNTRL	398681	101494	3.03	11.1	1.83	8.8
MAP-RA	1657472	483853	2.89	12.5	2.14	11.8

The decrease of the mean and the RMS of the analysis departure with respect to the background departure is an indication of the favourable influence these observations have in the analysis.

5 Assimilation and model diagnostics

For many MAP case-studies mesoscale model simulations have been performed using ECMWF operational analyses as initial and boundary conditions (e.g. Richard et al., 2003 and Volkert et al.,2003). Thus, the following comparisons of the 'new' MAP-RA with the 'old' OPER'99 allow for an estimation of the overall differences between both analyses, while the comparisons of MAP-RA with CNTRL and NOPRO enable an assessment of the impact of additional MAP observations.

5.1 Analysis increments of geopotential height

Analysis increments are calculated by subtracting the background field from the analysis. Small RMS analysis increments are a sign of consistency of the short range forecast with the observations. In Fig. 6, the differences of RMS of analysis increments for the geopotential at 500 hPa are presented. First, the MAP-suite has everywhere smaller increments than OPER'99 (bluish colours in Fig. 6a). This positive impact of the MAP-suite becomes most obvious across the Atlantic and Northern Africa, regions which benefit from the better use of satellite data. Second, the additional MAP observations have a negligible influence on the 500 hPa geopotential (Fig. 6b; values of less than 2 m, which is below the contour threshold in Fig. 6a). In terms of analysis increments of geopotential, the impact of the MAP-suite is clearly exceeding the impact of additional MAP observations. Similar impact has been seen for the other model variables.

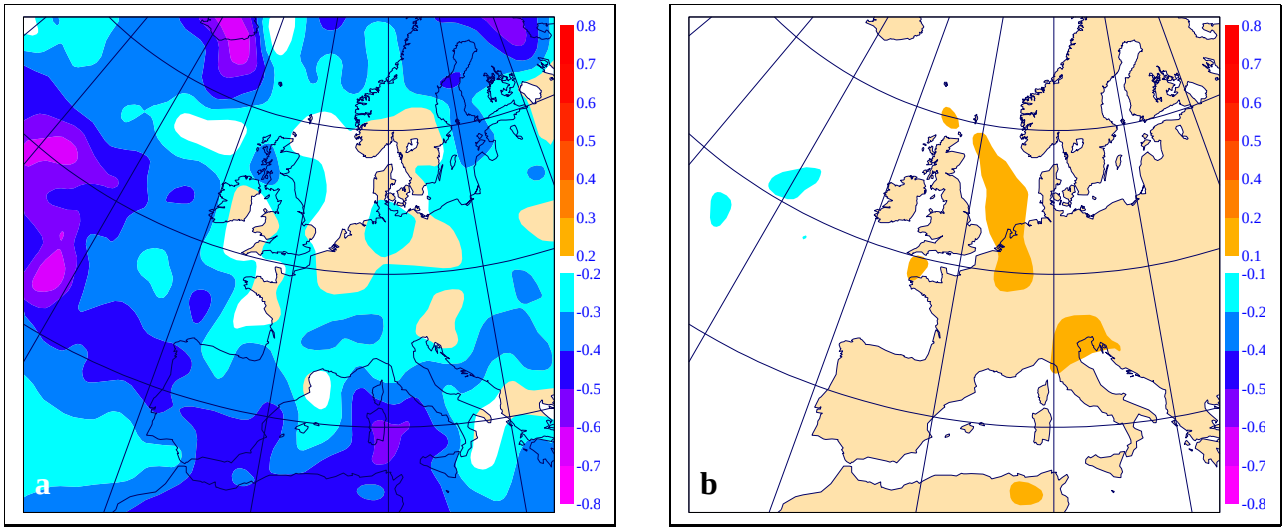

Figure 6: Differences of RMS of analysis increments for the geopotential [dam] at 500 hPa between (a) CNTRL and OPER'99 and (b) MAP-RA and CNTRL calculated for the SOP.

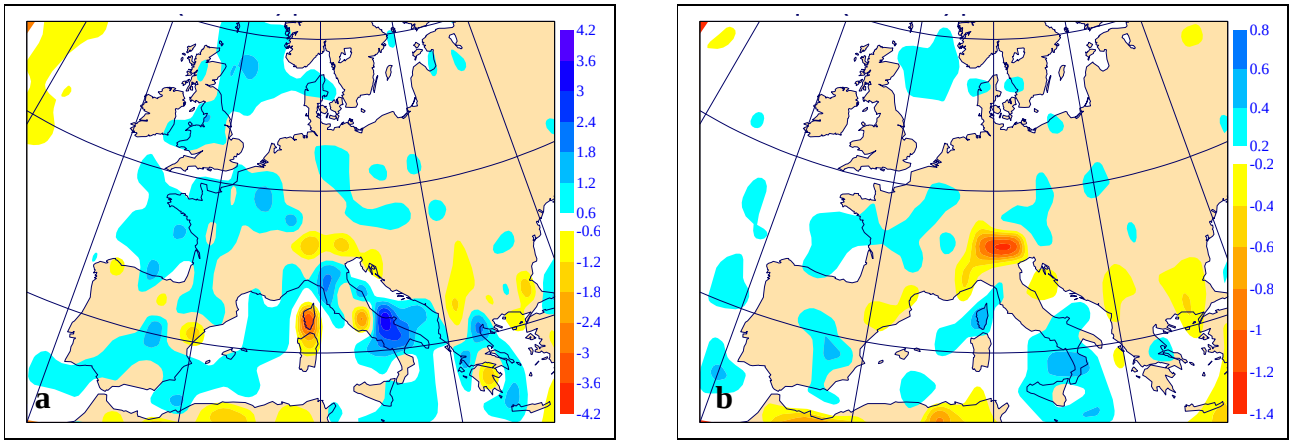

Figure 7: Mean analysis differences of (a) the total column water vapour [kg/m^2] and (b) specific humidity [g/kg] at 850 hPa between MAP-RA and OPER'99 averaged over the entire SOP.

5.2 Analysis differences of integrated water vapour and specific humidity

Now we focus on the humidity distribution of the different analyses. The mean analysis differences of the vertically integrated (total column) water vapour (IWV) show predominantly more humid conditions in MAP-RA than in OPER'99 (Fig. 7a). Locally, the differences are generally less than $1.2\,kg/m^2$, corresponding to about 7 % of the mean integrated water vapour content over Europe ($17\,kg/m^2$ for the SOP). However, in mountainous regions like the Alpine crest and Corsica regions MAP-RA is slightly drier than OPER'99.

In the boundary layer, the spatial distribution of the mean humidity differences resemble the IWV patterns, slightly moister across northwestern Europe and the Mediterranean Sea and slightly drier across the Alps and the Balkan (Fig. 7b, specific humidity difference at 850 hPa). These drier conditions across mountainous regions are partly caused by the increased model resolution resulting in a higher model orography in the MAP-suite than in OPER'99.

The influence of MAP observations becomes evident in the analysis differences in Fig. 8. First, we compare MAP-RA with CNTRL. The IWV differences (Fig. 8a) as well as the differences of specific humidity in the boundary layer (Fig. 8b) show that MAP-RA is moister across France and Italy. Particularly, across southeastern France and the adjacent Gulf of Lion, MAP-RA is more than $1\,kg/m^2$ IWV moister than CNTRL, with the largest differences in the lower levels (exceeding $1\,g/kg$ for the specific humidity at 925 hPa, not shown). The moister conditions in the Po valley region are noteworthy (see section 6.2). Across the western Mediterranean Sea close to Sardinia and along the French-German border MAP-RA is drier than CNTRL.

Which role did European windprofiler play? To answer this question, an additional analysis experiment was performed for the first month of the SOP excluding all European windprofiler information only (NOPRO). In Fig. 8c,d the mean humidity differences between MAP-RA and NOPRO are displayed. Generally, the differences are small, amounting to less than $0.6\,kg/m^2$ for the IWV content and less than $0.3\,g/kg$ for the specific humidity in the boundary layer. Obviously, the European windprofilers are hardly responsible for the large differences between the MAP-RA and CNTRL in the Gulf of Lion region. However, windprofilers seem to dry the troposphere in the southern Alpine region and to moisten the Adriatic Sea and southern Italy (Fig. 8d). This feature is also present in Fig. 8b which confirms the windprofilers influence in MAP-RA over these areas.

In summary, MAP observations lead to moister conditions in the Po valley region, despite the fact that the additional wind observations provided by European windprofilers tend to dry the troposphere in this region. Also, a moister humidity field can be seen across southern France and the Adriatic Sea.

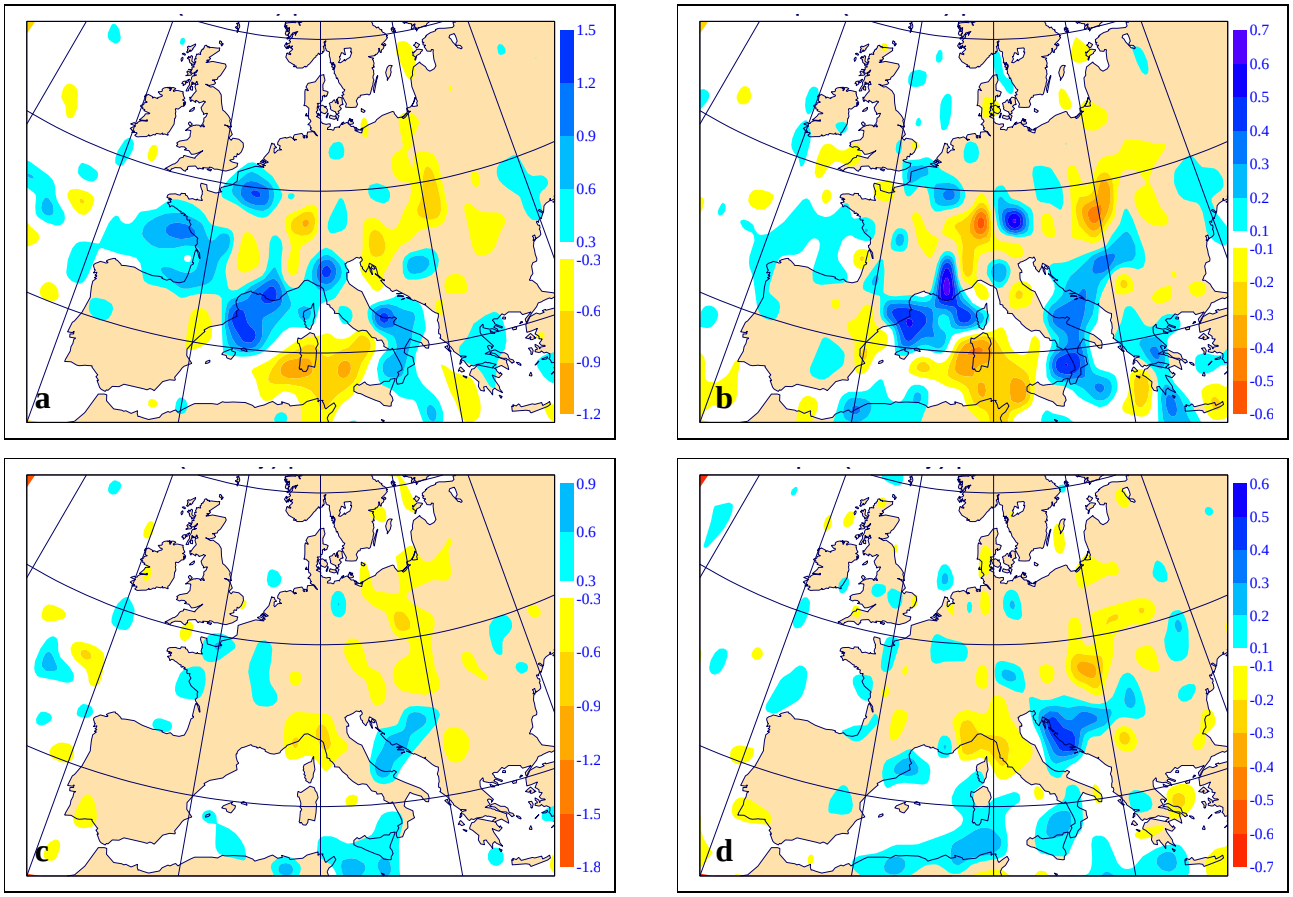

Figure 8: Mean analysis differences between MAP-RA and CNTRL (a,b) and between MAP-RA and NOPRO (c,d) of the total column water vapour [kg/m^2] (a,c) and specific humidity [g/kg] at 850 hPa (b,d) averaged over one month starting on 7 Sep 99.

5.3 Forecast impact

In terms of forecast impact, MAP-RA is better than CNTRL after day 3. The geopotential anomaly correlation scores at different pressure levels (850, 500 and 200 hPa), verified against the own analysis and radiosonde observations indicate a slight positive impact over North Atlantic, North America and North Pacific (not shown). However, it was not the prime objective of MAP to improve the forecast. In fact, MAP observations only supplement the existing observing system, which is already very dense across Central Europe.

6 Results on some specific IOPs

After investigating the quality of ECMWF's precipitation forecast during the full SOP, we focus on some special IOPs in this section. Additional IFS experiments have been performed for specific periods to complement the investigations and allow for an estimation of the impact of certain observation types available during the SOP and used in the MAP-RA.

6.1 Precipitation in the Po Catchment

Daily precipitation (24 hour accumulations from 06 UTC onwards) in the southern Alpine Region, an area comparable with the catchment of the Po river (7 - 12 ° E and 45 - 46.5 ° N), are presented here. Observed precipitation values for validation are taken from high resolution (25 km) analyses of daily Alpine rain-gauge observations embracing roughly 5000 rain-gauges (Frei and Häller, 2001; Frei and Schär, 1998). The forecast rainfall is based on the model forecast started at 12 UTC (*i.e.* + 18 - 42 h forecast range). Figure 9 depicts the time series of daily precipitation averaged over the Po catchment area (66.000 km^2) for observations, OPER'99, CNTRL and MAP-RA, respectively.

The agreement of the forecasts with the precipitation observations is remarkable. Peak values are found for IOP2b (20 Sept 99; day 13 in Fig. 9) recording 58 mm/day, IOP8 (21 Oct 99, day 44) and IOP15 (6 Nov 99, day 60) recording 30 mm/day. Generally the timing of the events is well represented in both suites. The forecast based on OPER'99 is performing well by capturing the majority of the events recording more than 10 mm area averaged precipitation. Forecasts from MAP-RA show a better agreement with observations, e.g. on days 8 and 40 the spurious rainfall predicted by the operational forecast is not present in MAP-RA. During the first month forecasts from CNTRL are similar to the ones of MAP-RA, however, the peak values of the heavy precipitation events in the latter half of the SOP are overestimated. The observed mean daily precipitation of 5 mm/day is reproduced by forecasts from MAP-RA, while forecasts from CNTRL overestimate the mean amount by 4 % and operational forecasts by 10 %.

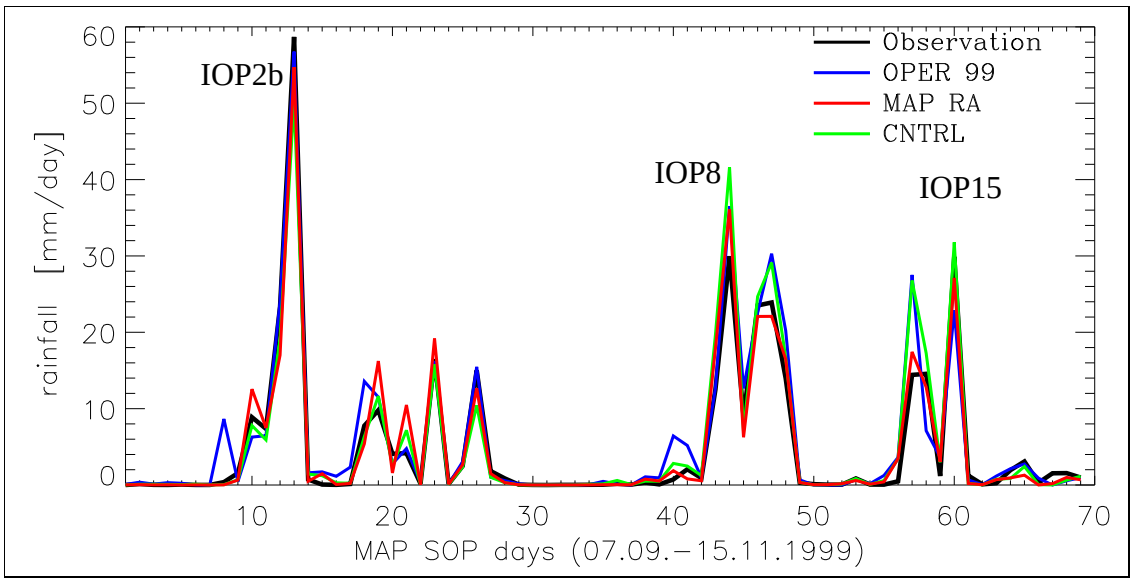

Figure 9: Time series of daily precipitation averaged over the Po catchment in the southern Alpine region. Rainfall data are taken from IFS forecasts initialized at 12 UTC and a forecast range of + 18 - 42 h.

6.2 IOP2a: 17 September 1999

During IOP2a on 17 Sep 99, a well defined squall-line crossed the Lago Maggiore area, where seven ground-based research radars provided detailed observations. Numerical simulations of this convective event have been performed with the Mesoscale Model Meso-NH by using a threefold nesting technique with horizontal mesh-sizes of 32, 8 and 2km (Lascaux et al., 2003). The reference experiment initialized with OPER'99 analysis on 17 Sep 99 12 UTC succeeds reasonably well to initiate the convective line over the Alpine foothills and to reproduce its propagation towards the East (Fig. 10c,d). However, initializing the Meso-NH Model with the MAP-RA, convection is almost entirely inhibited in the mesoscale simulation (Fig. 10e,f).

In the following we focus on the analyzed humidity field to detect, for this episode, the failure of convection in the mesoscale simulation. The analysis difference of specific humidity (Fig. 11) shows that the MAP-RA at 850 hPa is $5 g/kg$ drier than CNTRL in the southern Alpine region centered around 10 ° E. This is opposite the earlier finding that on average the MAP-RA is slightly moister in this region (comp. Fig. 8b).

The lack of humidity becomes apparent in the zonal vertical cross sections along 45.7 ° N slicing the southern foothills of the Alps at 12 UTC (Fig. 12). Just east of Milano, between 9 and 11 ° E, the region were the squall-line occurs, there is a dry tongue of air with less than $6 g/kg$ specific humidity extending down to 900 hPa (Fig. 12a). This dry region, extending well into the boundary layer, is neither present in CNTRL nor in OPER'99 (Fig. 12b,d). However, there are differences in the low-level humidity content between OPER'99 and CNTRL: moister conditions near Milano and drier conditions across the Adriatic Sea in OPER'99. The difference between MAP-RA (Fig. 12a) and NOPRO (Fig. 12c) is caused by the use of windprofiler data in the MAP-RA which tend to dry the troposphere (see section 5.2). The differences are largely confined between 9 and 11 ° E, close to the location of the Lonate windprofilers (45.6 N, 8.7 E).

To highlight the moisture evolution during the afternoon of 17 Sep, when the squall-line was sweeping across the Lago Maggiore area, the observed Milano radiosonde is compared with corresponding analyzed humidity profiles in Fig. 13. At 12 UTC, the time the mesoscale simulation has been initialized, the humidity profile of OPER'99 is too wet for the entire troposphere. The observed profile (in black thinned high resolution profile is depicted) shows high values (more than $10 g/kg$) below 950 hPa and relatively low ones (less than $5 g/kg$) around 800 hPa. In the following hours (18 UTC) the humidity has risen up to 900 hPa, while the dry layer around 800 hPa decreased. 6 hours later, just after the squall-line has passed Milano releasing heavy precipitation, the specific humidity in the mixed boundary layer amounts to $8 g/kg$. The analyzed humidity fields do not reflect the observed profile. While OPER'99 is generally too moist (green line), the MAP-RA (red line) fails to reproduce the correct humidity profile. In fact, at 12 UTC, the humidity is too low below 850 hPa and at 18 UTC the dry profile has been extended throughout the boundary layer below 750 hPa.

In Fig. 14a, the time-height diagramme of vertical motion valid at Lonate (the nearby location of two windprofilers) is depicted. Between 12 and 21 UTC, subsidence encompasses the entire troposphere ($1 Pa/s$ at 700 hPa at 15 UTC) in the MAP-RA. In CNTRL, the subsidence is limited to the lower troposphere (Fig. 14b) and it decreases later in the evening (21 UTC). In NOPRO, descending motion is present between 12 and 18 UTC in the lower troposphere, like in CNTRL. However, enhanced vertical motion develops after 18 UTC, with subsidence in the mid-troposphere at first followed by upward motion in the lower troposphere (Fig. 14c).

Intercomparison of the humidity profiles and the vertical motion fields between the MAP-RA, CNTRL and NOPRO demonstrates once again the impact of windprofiler, in particular on the humidity field. Throughout the afternoon of 17 Sep, the MAP-RA is considerably drier than NOPRO (Fig. 13). The Lonate windprofilers have modified the wind field by leading to enhanced subsidence.

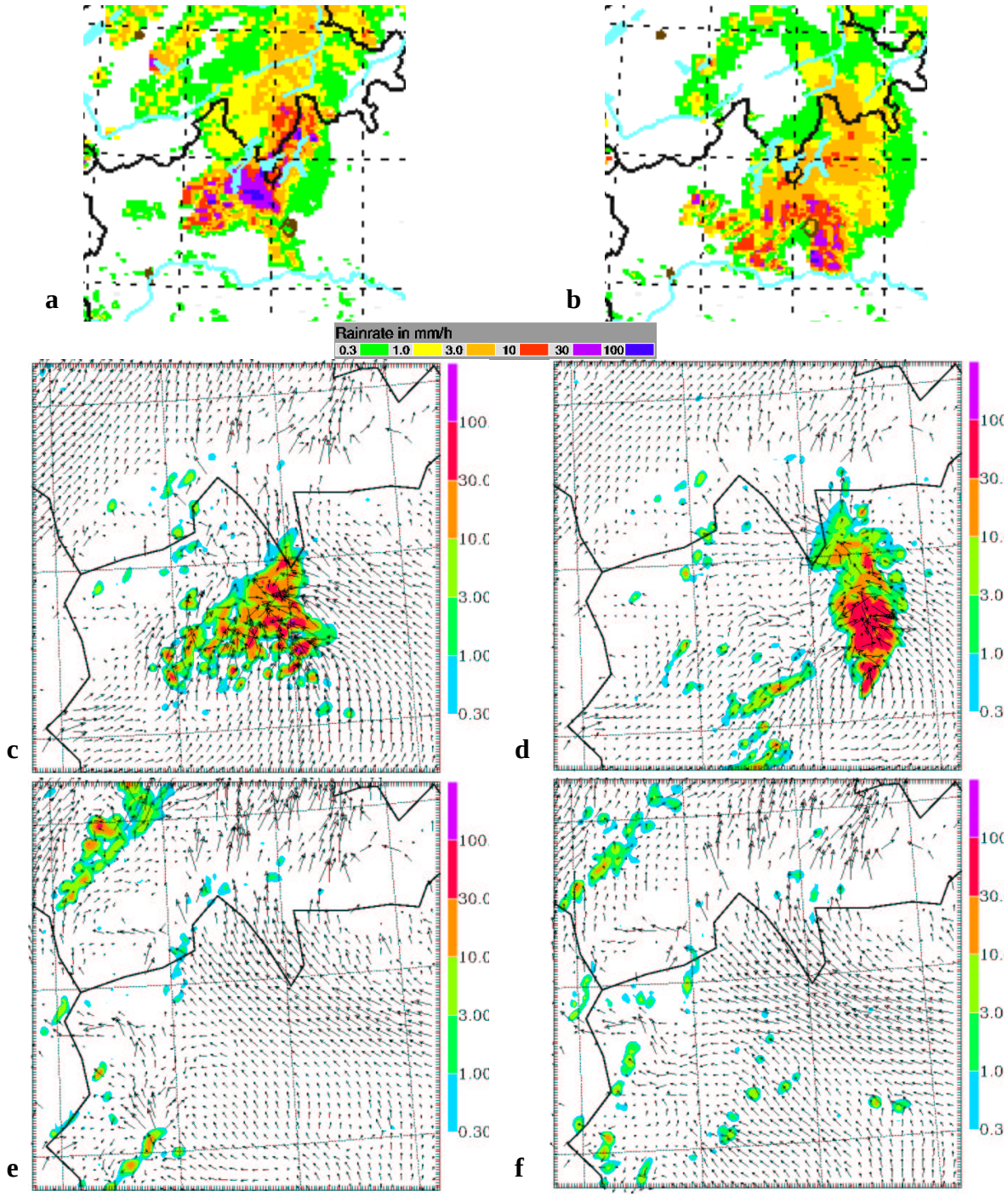

Figure 10: Radar observed (a,b) and Mesoscale Model forecast (c-f) precipitation fluxes at 21 UTC (a,c,e) and 23 UTC (b,d,f) on 17 September 99 across the Lago Maggiore Area in northwestern Italy (domain size 250×250 km^2). The Meso-NH has been initialized at 12 UTC with OPER'99 (c,d) and with MAP-RA (e,f). The forecast precipitation fluxes and wind arrows depict model fields 2000 m above ground (Meso-NH images by courtesy of E. Richard).

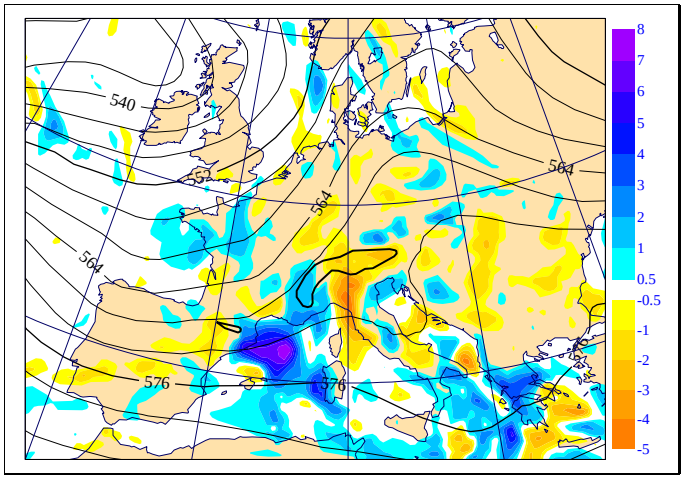

Figure 11: Analysis difference of specific humidity at 850 hPa between the MAP-RA and CNTRL (colour coded) superimposed with 500 hPa geopotential height at 12 UTC on 17 Sep 99.

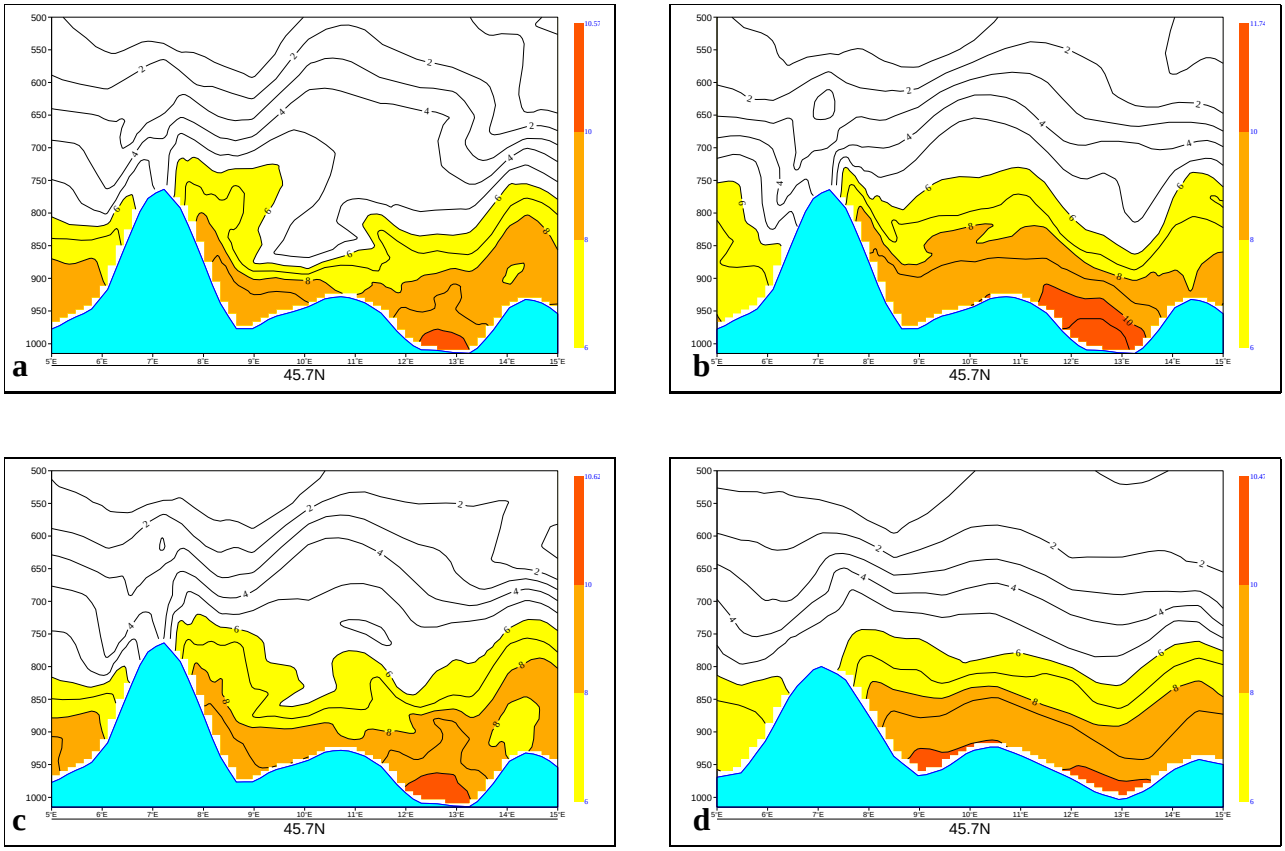

Figure 12: Vertical cross-section of specific humidity along 45.7 N at 12 UTC on 17 Sep 99 for (a) MAP-RA, (b) CNTRL, (c) NOPRO and (d) OPER'99.

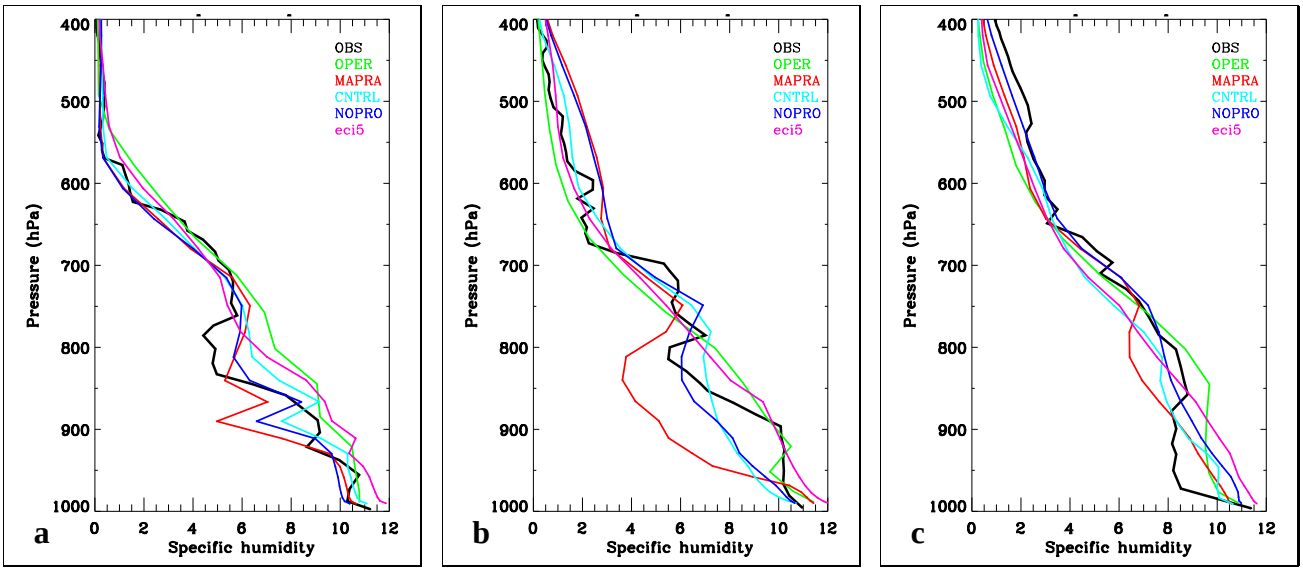

Figure 13: Intercomparison of humidity soundings for Milano at (a) 12 UTC, (b) 18 UTC and (c) 00 UTC on 17 and 18 Sep 99, respectively: observation (black), OPER'99 (green), MAP-RA (red), CNTRL (light blue), NOPRO (dark blue) and experiment eci5 (magenta).

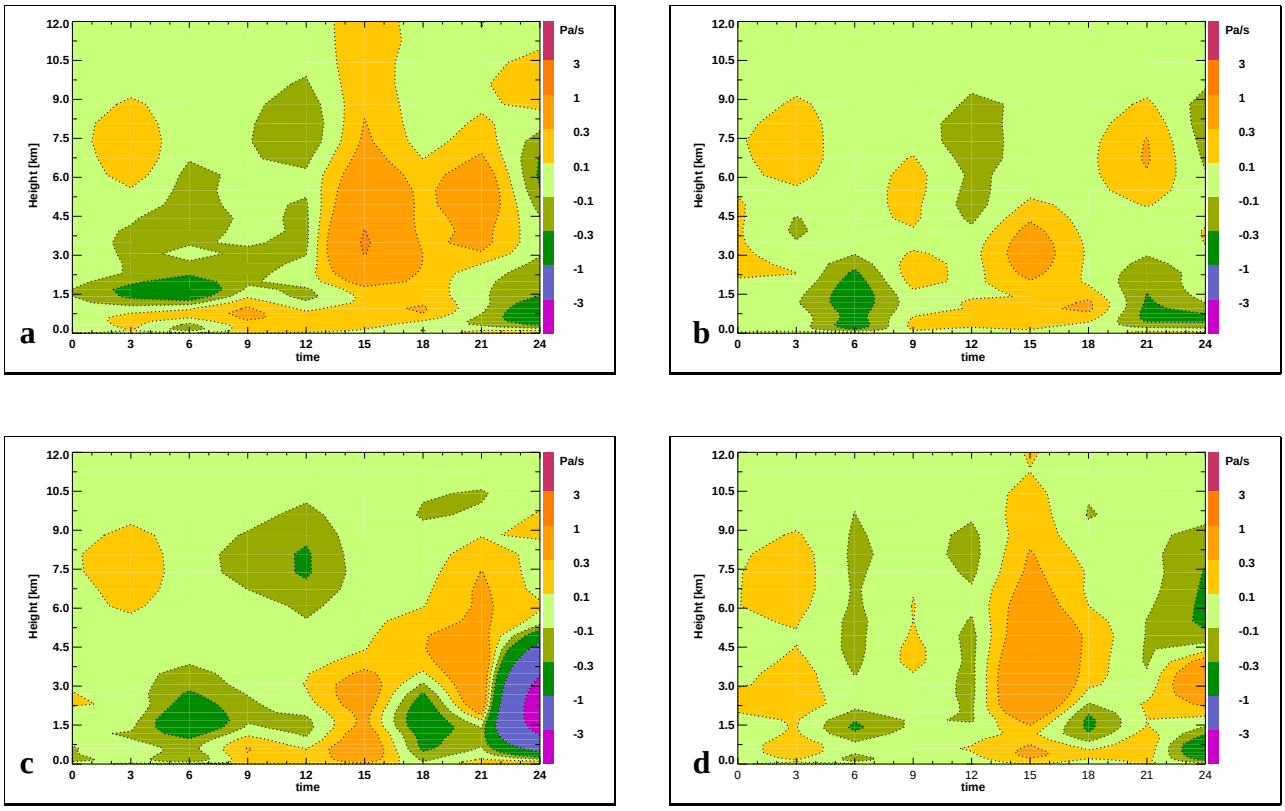

Figure 14: Time-height diagramme of the vertical motion at the location of the windprofiler Lonate (45.6 N, 8.7 E) for (a) MAP-RA, (b) CNTRL, (c) NOPRO and (d) experiment eci5 on 17 Sep 99. Note that descent is colour-coded yellowish-red and ascent greenish-blue.

A coupling between mass and humidity fields in 4D-Var can be induced by the model dynamics but also through the specific humidity background error standard deviation calculation. Operationally, an empirical formula computes at every cycle the humidity standard deviation as a function of background temperature and relative humidity. Modifications of the wind field due to windprofilers affect the temperature and via that formula also the humidity field.

To prove that, we performed an experiment in which a constant humidity background error standard deviation was used instead of being computed by the empirical formula. For IOP2a, this special analysis experiment (Exp-ID: *eci5*) was started with MAP-RA initial conditions. The same European windprofilers were assimilated as in MAP-RA. Comparison between MAP-RA and *eci5* analyzed humidity profile at Milano shows remarkable differences (red and magenta lines in Fig. 13) while the vertical motion field has hardly changed (Fig. 14a,d). In both cases the assimilation of the Lonate windprofiler enhances subsidence in the Lago Maggiore region. However, this has different consequences on the humidity resulting in considerably moister conditions in the experiment using a constant humidity background error standard deviation. Evidently, the descending motion indirectly feeds back on the humidity field through variations in the humidity background error standard deviation (MAP-RA; dry conditions) but not directly through adiabatic drying (experiment *eci5*; moist conditions). For IOP2a, the errorneous feed back causes the low humidities.

6.3 IOP2b: 20 September 1999

As we have already seen in the rainfall time series for the Po catchment (Fig. 9), IOP2b constitutes the heaviest precipitation event recorded during the SOP. While the forecast daily rainfall accumulation integrated over the

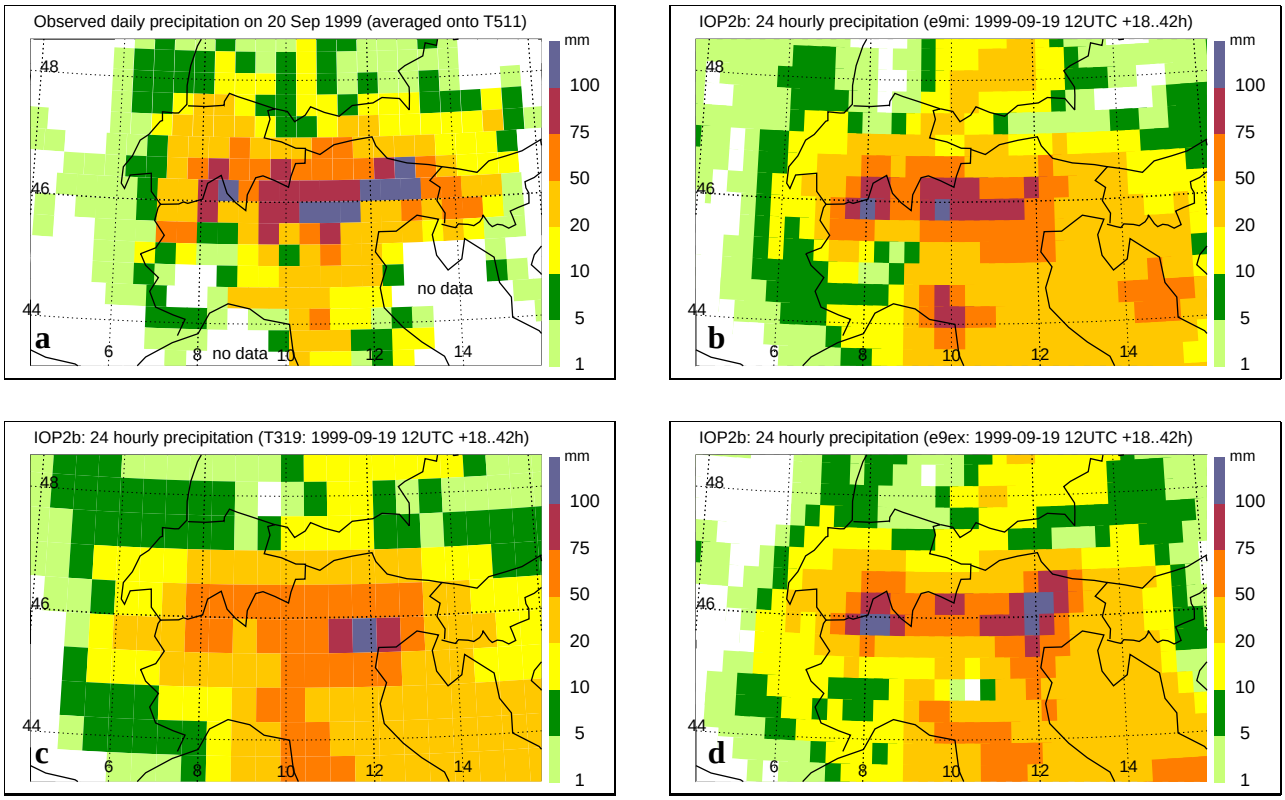

Figure 15: Daily accumulated precipitation for IOP2b (20 Sep 99, 6 UTC - 6 UTC): (a) analyzed precipitation based on gauge observations and projected on T511 grid, (b) T511 forecast starting from MAP-RA, (c) operational T319 forecast from OPER'99 and (d) T511 forecast from CNTRL.

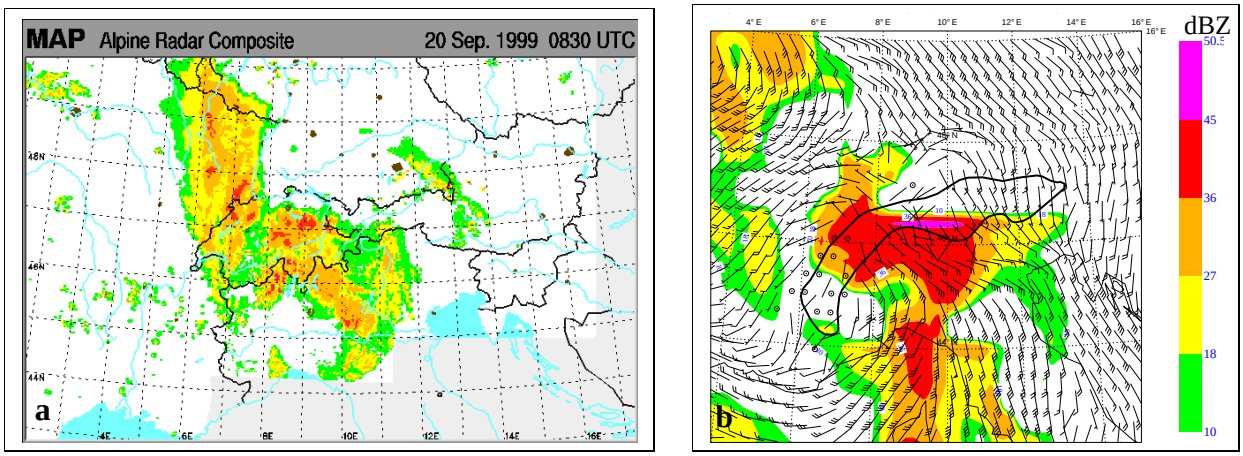

Figure 16: Observed and synthetic radar reflectivity on 20 Sep 99: (a) Alpine Radar Composite depicting observed instantaneous radar reflectivities at 8:30 UTC and (b) synthetic radar reflectivity 2000 m above ground (same colour coding) collocated with the low level wind field in 925 hPa valid at 9 UTC (1909199912 + 21h).

Po catchment area hardly differs from precipitation data (58.7 mm observed, 56.7 mm forecast from OPER'99 and 54,7 mm forecast from MAP-RA; Fig. 9), there are differences in the rainfall's spatial distribution. In Fig. 15a, the daily accumulated precipitation from the gauge based precipitation analysis (Frei and Häller, 2001) projected onto the model grid is displayed. Strongest rainfall peaking in more than 100 mm was recorded in the Lago Maggiore area, in the Dolomites and Carnic Alps in northeastern Italy. Generally, intense precipitation with daily accumulations of more than 75 mm was observed in a 100 km broad belt along 46 ° N at the southern foothills of the Alps.

A zone of stronger precipitation along the southern foothills of the Alps is recognisable in all forecasts, in particular in the T511 forecasts. Forecast from OPER'99 misses the strong rainfall in the Lago Maggiore area but includes the precipitation maxima close to the Dolomites (Fig. 15c). Forecast from CNTRL reproduces the heavy precipitation exceeding 100 mm in the Dolomites and in the Lago Maggiore area (Fig. 15d), while MAP-RA predicts precipitation maxima in the Lago Maggiore area and the Bergamese Alps (Fig. 15b), both in good agreement with observations. The high rainfall values in northeastern Italy are missed by MAP-RA forecast. Unfortunately there are no humidity radiosoundings available in this region (e.g. Udine) to investigate this forecast failure. All forecasts overestimate the precipitation north of the Alps by exceeding 10 mm in Bavaria. Here the lee-effect of the Alps is underestimated. Furthermore, MAP-RA reproduces the 'dry' area East of the Alps Maritime in Liguria, confirmed by the high resolution analysis.

The collocation of an observed radar image with its synthetic counterpart highlights to which degree of realism it is possible to match qualitatively individual precipitation systems using forecast fields of the IFS global model (Fig. 16). The synthetic radar reflectivities are calculated with a simple formula, which uses fields of rain water, cloud water and ice to construct radar echoes (Fovell and Ogura, 1988).

Visualized by the wind field at 925 hPa, the moisture-laden cyclonic airflow is impinging on the Appennines and the Alps, where at the luv-slopes high rainrates exceeding 10 mm/h (> 36 dBZ) at 2000 m are forecast (Fig. 16b). The strongest rainrates with more than 30 mm/h (> 45 dBZ) are predicted at the southern Alpine slopes, where the flow in an unstable atmosphere is orographically forced to rise over the mountain chain. One branch of the precipitation system extends northwestward across Switzerland into France. The general features of this precipitation system can be identified in the radar observations (Fig. 16a), *i.e.* the cyclonic curl of the rainfall area south of the Alps and its extension towards France. However, the remotely-sensed precipitation intensity hardly exceeds 10 mm/h. The precipitation area upstream of the Appennines is not within the range of the Italian radars.

6.4 IOP8: 21 October 1999

On 21 Oct 99, another heavy rainfall event occurred in the southern Alpine region. During IOP8, the daily precipitation is quite uniformly distributed throughout the Po catchment area and the adjacent Alpine foothills amounting to 20-50 mm (Fig. 17a). Heaviest precipitation with maxima exceeding 50 mm were recorded in the area of Milano. All model forecasts, T319 operational forecast and T511 forecasts from MAP-RA and CNTRL, reproduce the widespread rainfall surmounting 20 mm south of the Alps. The higher resolution forecasts from MAP-RA and CNTRL predict high precipitation accumulations for the Milano region (Fig. 17b,d) well matching the observed pattern. However, all forecasts overestimate the precipitation over the western Appennines. The spurious rainfall peak predicted by the T511 forecast from CNTRL in the foothills of the Dolomites, which leads to the overestimation of the mean rainfall averaged over the Po catchment (see Fig. 9), is removed in MAP-RA.

Medina and Houze (2003) showed, that the strikingly different precipitation patterns of IOP2b and IOP8 correspond with different flow regimes: unblocked flow up and over the mountains during IOP2b and flow around or blocked during IOP8. Although forecasts from MAP-RA do not agree in every way with precipitation data, they do capture the main difference between IOP2b and IOP8 (Fig. 15a,b and Fig. 17a,b, respectively) and so, document the capability of the model to reproduce the different mesoscale flow situations.

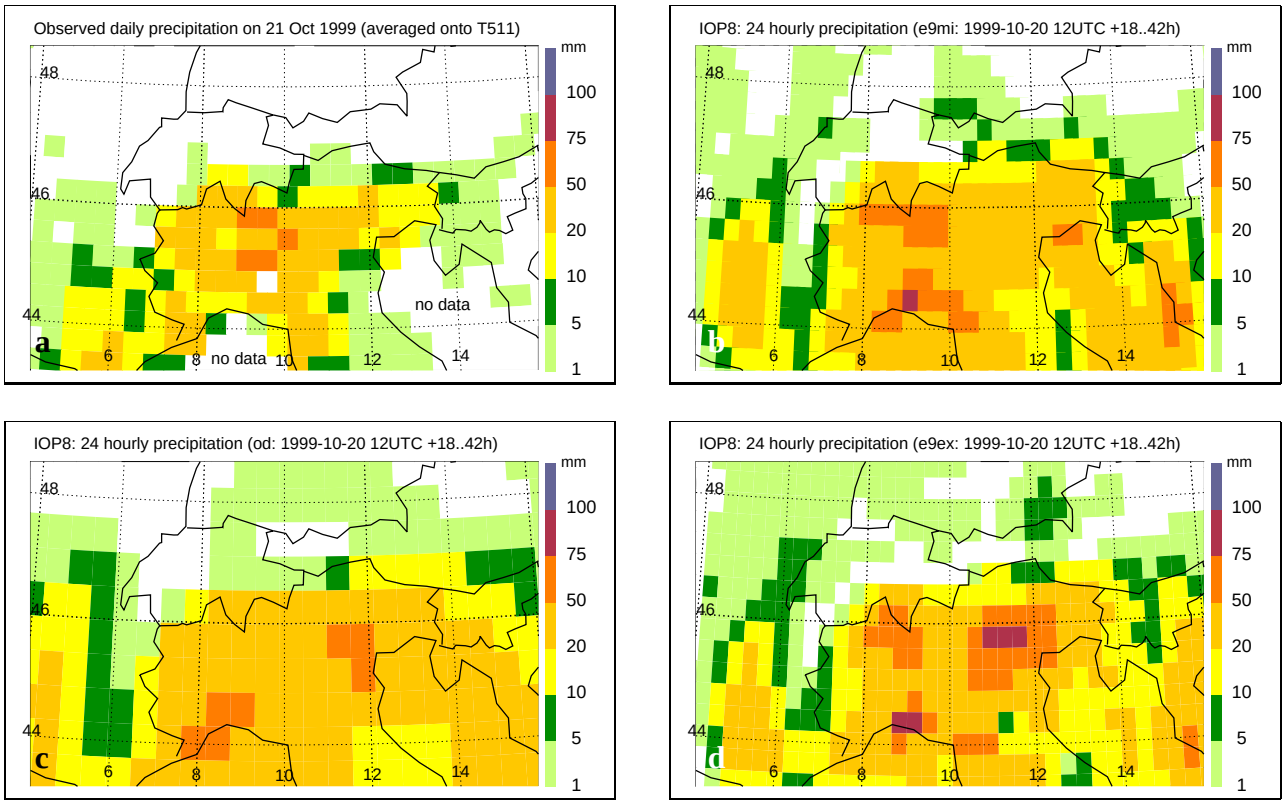

Figure 17: Daily accumulated precipitation for IOP8 (21 Oct 99, 6 UTC - 6 UTC): (a) precipitation analysis based on gauge observations projected on T511 grid, (b) T511 forecast from MAP-RA, (c) operational T319 forecast from OPER'99 and (d) T511 forecast from CNTRL.

6.5 IOP15: 6/7 November 1999

In contrast to the previously discussed cases, we focus on dynamical features for IOP15, though 30 mm/day area-averaged precipitation is well captured by MAP-RA. This case constitutes a good example of upper-level features, which were observed with ground-based and airborne remote-sensing instruments deployed during the MAP campaign. On 6 Nov, a trough was elongating meridionally from the North Sea to the Mediterranean Sea. The following day, this trough crossed the Alps forming a cut-off low at its southern end above Italy.

Based on NWP guidance, a flight pattern was planned (DLR-Falcon aircraft) to measure cross-streamer curtains of water vapour along this tropopause fold on 6 Nov. With the on-board H_2O-Dial instrument, low humidities in the lower stratosphere and upper troposphere were measured applying a technique described in Ehret et al. (1999). Fig. 18a shows very dry stratospheric air intruding the troposphere, marked by low humidity values of less than 50 ppmv reaching down to approximately 7 km altitude between 15 and 16 UTC.

A corresponding image of reanalyzed humidity is given in Fig. 18b, displaying the humidity in a vertical cross-section along 45 ° N extending from Bordeaux to Venice at 15 UTC. Very low humidities of 50 ppmv extend down to 600 hPa (corresponding to 4 km altitude), giving evidence of the tropopause fold and the intrusion of dry stratospheric air. A closer inspection allows to detect mesoscale similarities between H_2O-Dial observation and the MAP-RA; whereas the 40 ppmv isoline drops vertically in the upper troposphere by about 3 km at the western flank of the intrusion (at 3 ° E), it slants with an angle of about 45 ° at its eastern flank (at 4-8 ° E). A comparably good agreement of Dial observation and corresponding analysis is discernible neither in CNTRL nor in OPER'99 analyses (not shown).

Observations of ground-based remote-sensing instruments are presented in Fig. 19 using time-height diagrammes of horizontal wind velocity. The measurements of the VHF (Fig. 19a) and UHF (Fig. 19b) sensors of the Lonate windprofilers are displayed using a tiling method which enables the depiction of the actually measured data without any field smoothing. The length of the individual tiles represents the frequency of the measurements reported by the windprofilers, with 1 hourly data from VHF Lonate and quarter-hourly data from UHF Lonate. Data sparse areas are also easy to identify. The corresponding analysis and background wind fields of MAP-RA at Lonate are displayed using the same time-height representation (Fig. 20).

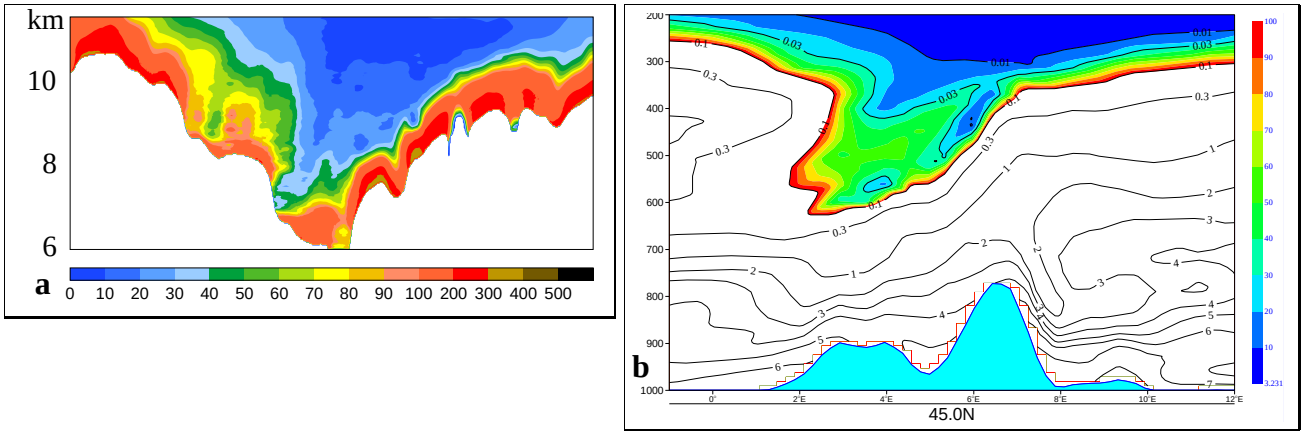

Figure 18: Section of low water vapour concentration across a tropopause fold; (a) data (in ppmv) obtained with an airborne H_2O-Dial looking down from 11 km. The flight segment is along 45 ° N from Bordeaux (1 ° W) to Venice (12 ° E) between 15 and 16 UTC on 6 Nov 99. Collocated is a vertical cross-section of MAP-RA humidity at 15 UTC along 45 ° N (b; isolines of specific humidity in g/kg).

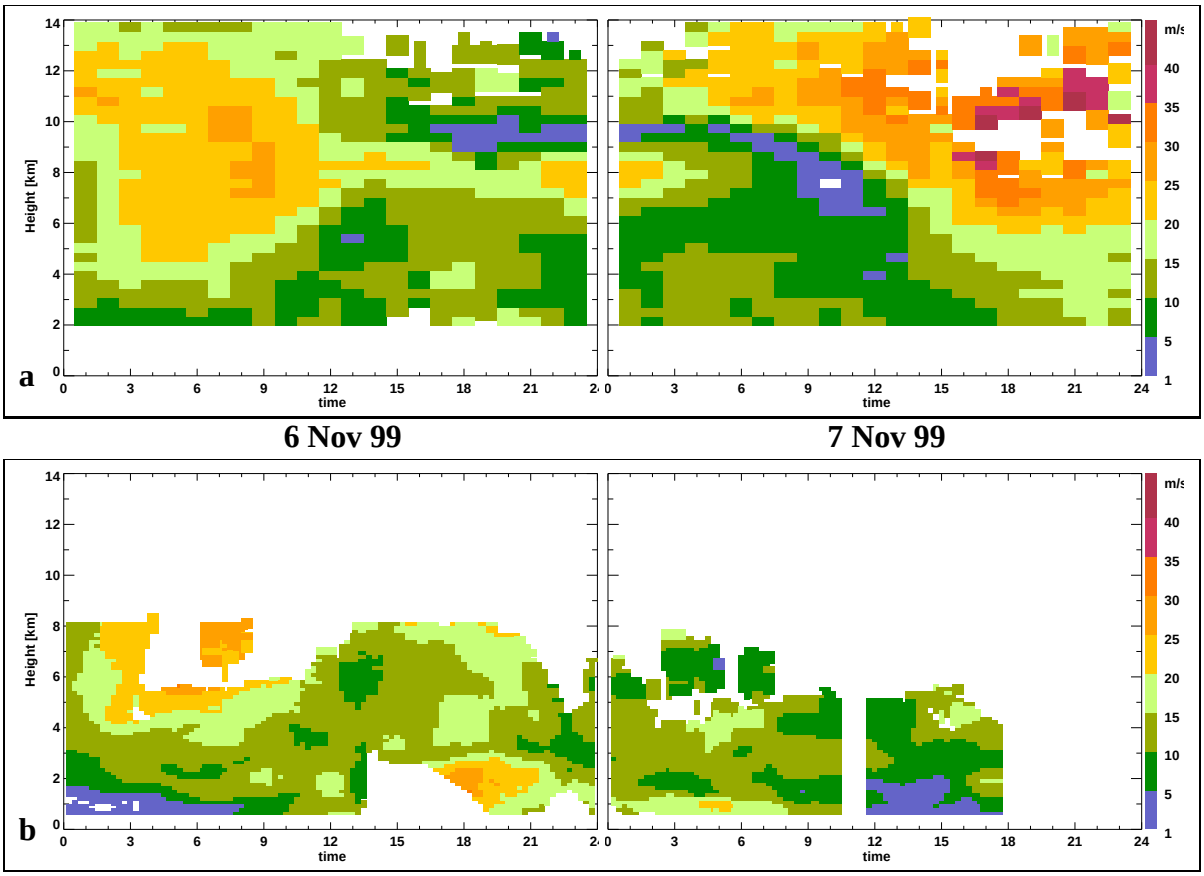

Figure 19: Time-height diagramme of horizontal wind velocity during IOP15 as observed by (a) VHF and (b) UHF windprofiler at Lonate.

The most prominent feature during IOP15 is the passage of the tropopause fold and the associated jet stream, which is crossing Lonate on 7 Nov. The wind in the upper troposphere strengthens considerably from 6 UTC onwards, first at higher levels ($z = 10$ *km*) and later in the mid-troposphere attaining values of 40 m/s at 10 km height and 20 m/s at 5 km at 18 UTC (right panel in Fig. 19a and 20a). Remarkably is the strong wind shear of 20 m/s/km between 8 and 9 km around noon on 7 Nov which is well captured in the background and analysis field (Fig. 20). Concatenated with the jet passage is a change in wind direction from slight southerly to blustery northerly wind. Also, the timing and the strength of the jet-stream passage is well captured by CNTRL and OPER'99 (not shown).

Another interesting feature is the formation of the north föhn associated with the passage of a cold front in the afternoon on 6 Nov. Documented by the UHF profiler, this north föhn event lasts for 15 hours (winds larger than 15 m/s below 3 km height; Fig. 19b). High wind velocities exceeding 20 m/s prevail from 17 to 21 UTC and are ceasing thereafter. However, the VHF profiler at Lonate which lowest measuring level is at 1.7 km height misses this low-level wind maximum completely (Fig. 19a). This has consequences for the MAP-RA. While the short-range model forecast captures the formation of the north föhn (background field in Fig. 20b), the vertical extent and the strength of the low-level wind are diminished in the analysis (Fig. 20a). Here the contradicting information of both Lonate windprofilers had to be compromised resulting in the decrease of the north föhn in MAP-RA. Exclusion of the windprofiler data retains the strong north föhn in the CNTRL analysis (not shown).

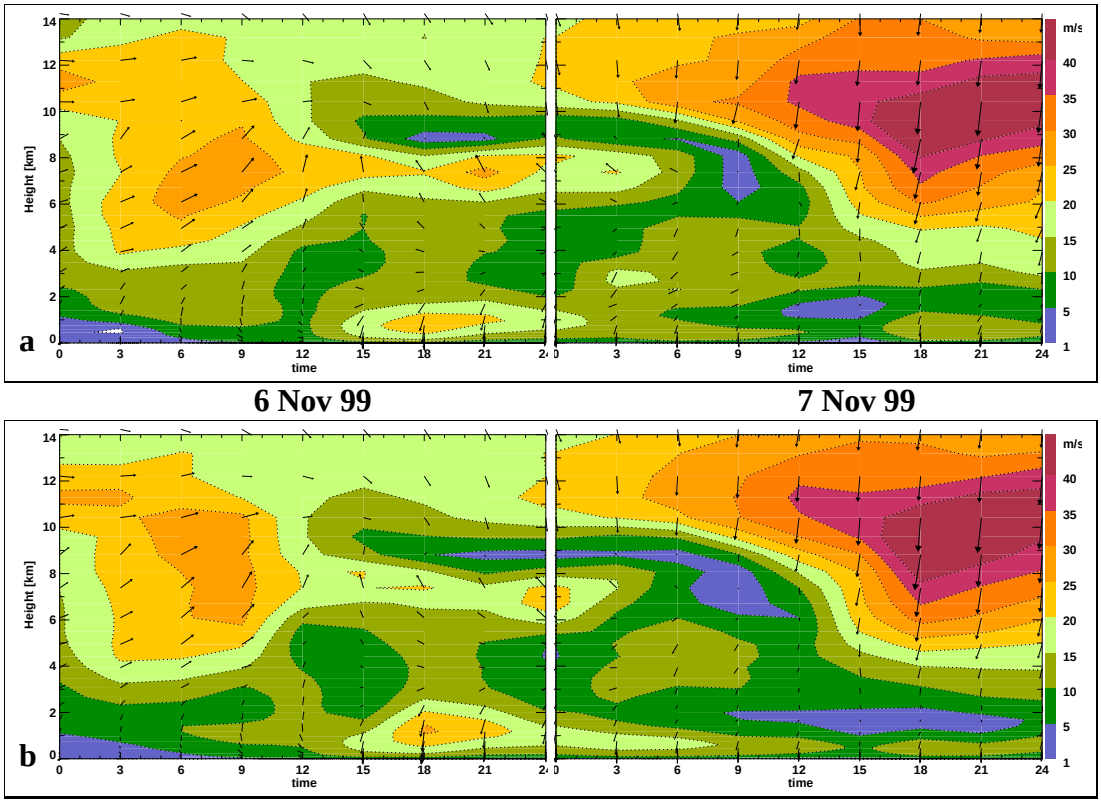

Figure 20: Time-height diagramme of the horizontal wind velocity of the MAP-RA during IOP15 at Lonate: (a) analysis and (b) background. The arrows indicate the direction of the horizontal wind.

The impact of the VHF profiler on the analysis is also visible in the location of the shear zone, where a southerly flow at lower levels alternates to a northerly flow aloft (in 9 km altitude from 6 Nov 12 UTC onwards; Fig. 20a). The windprofiler observations (Fig. 19a) compare better with the analysis than with the background of MAP-RA (Fig. 20), *i.e.* the strength of the southerly winds is increased (by about 5 m/s) and its location is lifted to about 8 km height in the analysis.

7 Validation using GPS based humidity measurements

In atmospheric processes, humidity is a highly variable parameter that plays a crucial role in atmospheric motions on a wide range of scales in space and time. Limitations in humidity observation accuracy, both its temporal and spatial coverage, lead to problems in predicting clouds and precipitation (e.g. IOP2a, section 6.2). Due to these limitations, the evaluation of humidity is also difficult. The emerging ground-based Global Positioning System (GPS) network gives the opportunity to validate the vertical integral of model humidity fields. Estimation of the integrated water vapor (IWV) in the atmosphere from the anomalous delays in the radio signal transmitted by the GPS satellites has an accuracy that is comparable to that of radiosondes (Bock et al., 2003) which are, at present, the primary data source of humidity vertical profiles.

The data has been retrieved from the MAGIC website[1]. In conjunction with software made available through the COST716 action, the measured Zenith Total Delay (ZTD) has been converted into IWV values at available

[1] *http://www.acri.fr/magic*

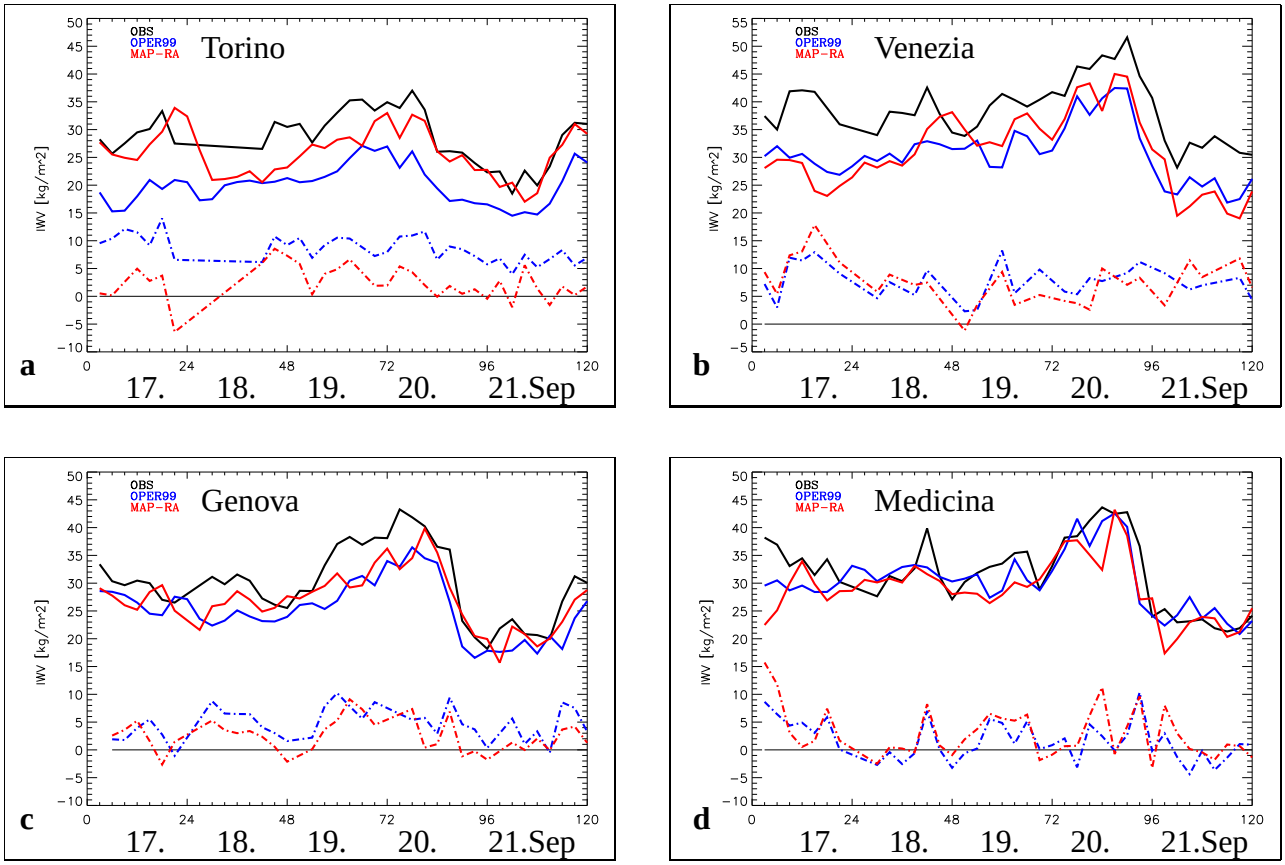

Figure 21: Time-series of GPS derived integrated water vapour observations (black) and analyzed counterparts of MAP-RA (red) and OPER'99 (blue) for (a) Torino, (b) Venezia, (c) Genova and (d) Medicina for the 5-day period starting on 17 Sep 99. The analysis departures (o-a) are depicted in dashed lines.

Alpine GPS stations. Time series of observed and analyzed IWV contents are presented for two 5-day periods (IOP2 and IOP8) at southern Alpine GPS stations (Figs. 21 and 22), together with an intercomparison of the spatial humidity distribution on 21 Oct during IOP8 (Fig. 23).

During IOP2 (17 to 21 Sep 99) the IWV content derived from GPS measurements is showing significant variations ranging from 20 to 50 kg/m^2 at the four Italian stations Torino, Genova, Medicina and Venezia (Fig. 21). The mean values are influenced by the station altitude and its proximity to the Mediterranean Sea. Highest IWV contents are recorded at all stations on 20 Sep, coinciding with the strong rainfall event of IOP2b (see section 6.3). These IWV maxima are succeeded by a sharp decrease by nearly 20 kg/m^2, progressing eastward from Torino (at 9 UTC; Fig. 21a) and Genova (at 12 UTC; Fig. 21c) to Medicina and Venezia at the Adriatic Coast (at 18 UTC; Fig. 21b,d).

Generally, the analyses are drier than the GPS observations with a mean deviation ranging from 1.6 to 8.5 kg/m^2 (for different stations and/or analysis). Whereas the main temporal evolution of the IWV content peaking during IOP2b is captured by the analyses, locally there are considerable differences between observations and analysis. One reason is the difference between station altitude and corresponding model height, e.g. the GPS station at Torino (eastern slopes of the Sea-Alps) has an altitude of 262 m above sea level, while in the MAP-suite this location is at 379 m and in OPER'99 even at 999 m altitude, resulting in a large systematic deviation between GPS observation and OPER'99 (Fig. 21a). Apart from this altitude effect, the analyses show the largest

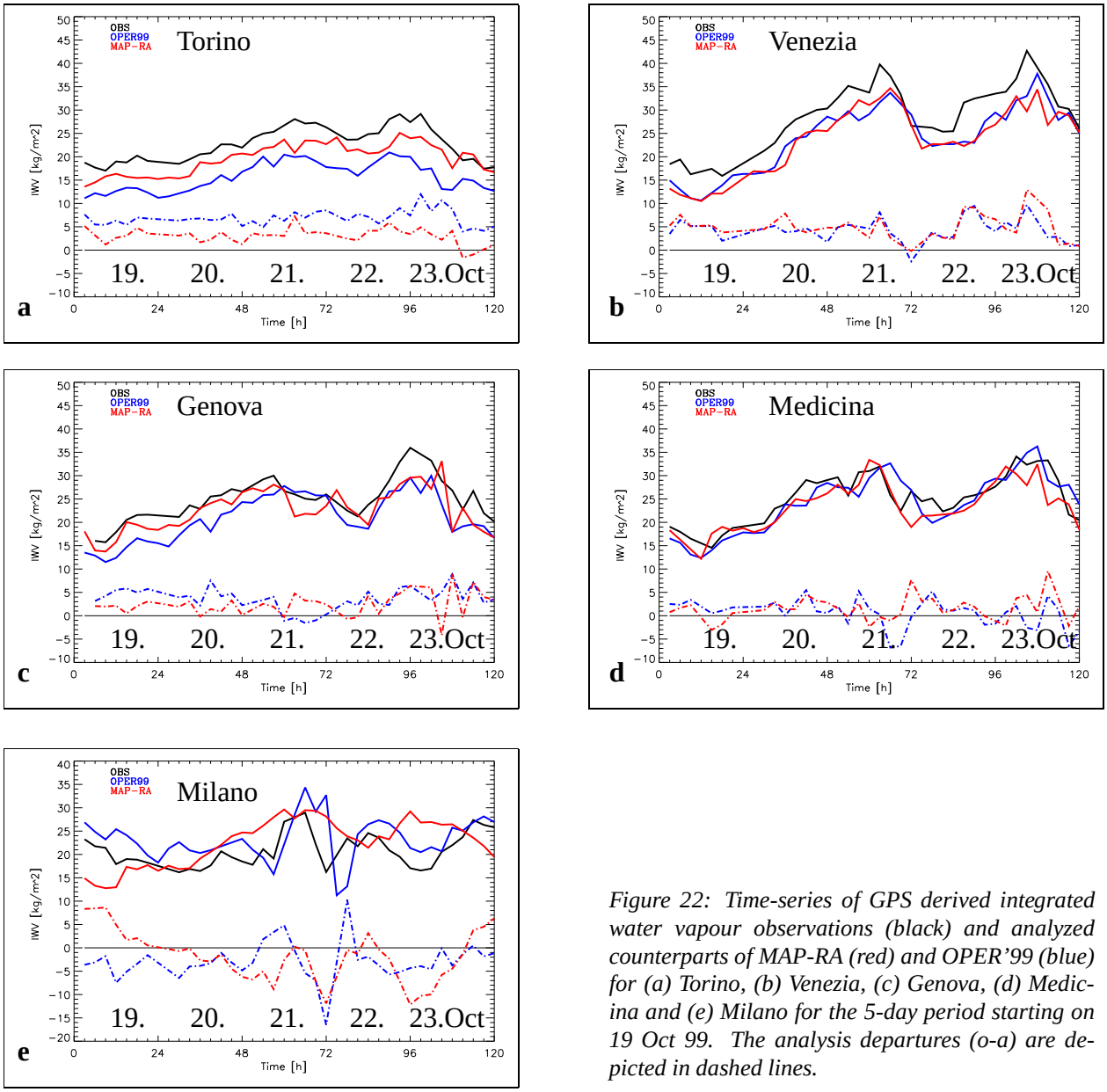

Figure 22: Time-series of GPS derived integrated water vapour observations (black) and analyzed counterparts of MAP-RA (red) and OPER'99 (blue) for (a) Torino, (b) Venezia, (c) Genova, (d) Medicina and (e) Milano for the 5-day period starting on 19 Oct 99. The analysis departures (o-a) are depicted in dashed lines.

deviations for the site of Venezia, close to the Mediterranean Sea, yielding a mean IWV difference of 7.5 kg/m^2 (Fig. 21b). Here the proximity to the warm SSTs of the Mediterranean Sea seems to be the main reason for the differences, where small changes in the boundary layer wind field can cause large deviations in humidity advection. The highest single observation-minus-analysis errors occur on 17 Sep (IOP2a), with the differences exceeding 10 kg/m^2, likely due to the meso-scale processes involved in the generation of the squall-line which cannot be resolved by the IFS (see section 6.2). Comparing the IWV observation-minus-analysis differences at the Italian stations during the 5-day period, MAP-RA shows a slightly better agreement with observations than OPER'99. However, given a GPS observation error of about 2 kg/m^2 (Bock et al., 2003), the intercomparison highlights the difficulties encountered to capture a realistic IWV content.

For IOP8 (19 to 23 Oct 99), the GPS derived IWV contents show large deviations for all stations south of the Alps (the Milano station, only available in Oct, is also added) within this 5-day period, with observed IWV changes of up to 200 % within 48 hours (Fig. 22). The two observed IWV maxima on 21 and 23 Oct are reproduced by both the MAP-RA and OPER'99. However, the analyses at the four 'MAGIC' stations (Torino,

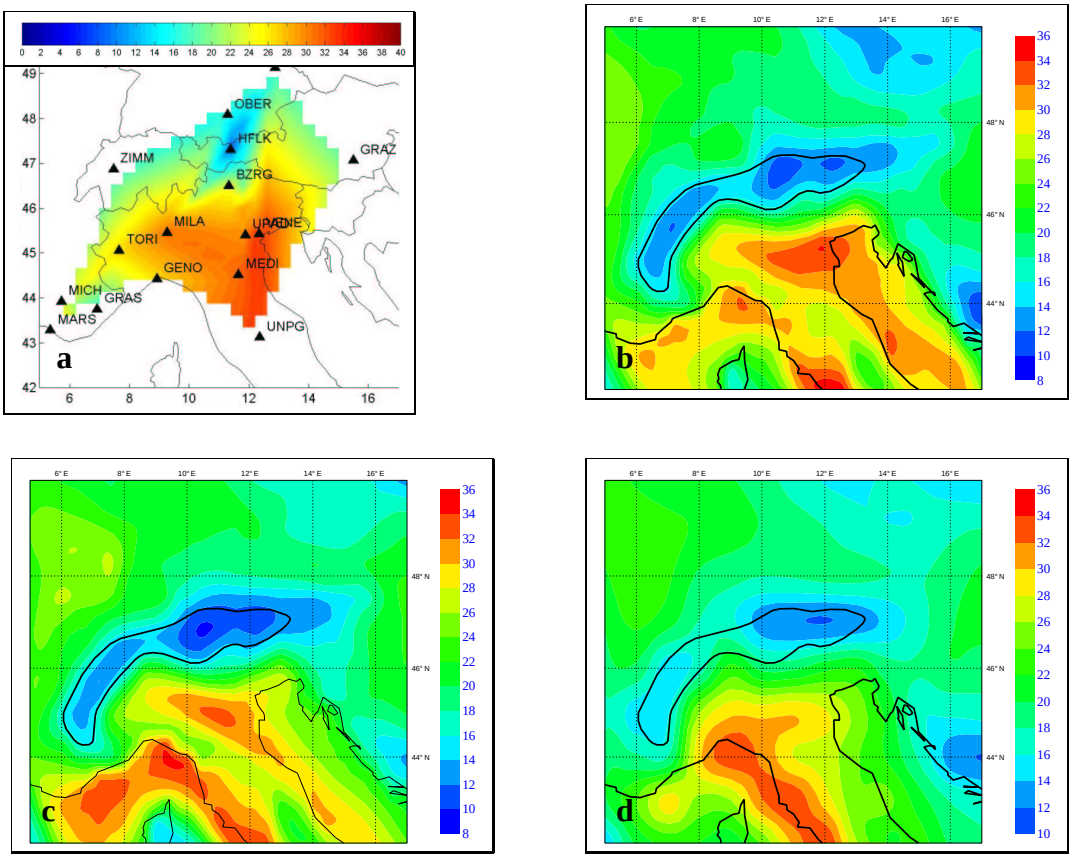

Figure 23: Integrated water vapour [kg/m^2] valid at 12 UTC on 21 Oct (IOP8): (a) GPS based observation, (b) MAP-RA, (c) CNTRL and (d) OPER'99 (Fig. 23a by courtesy of O. Bock).

Genova, Medicina and Venezia) are again too dry. In contrast, the experimental GPS station at Milano shows predominantly negative observation-minus-analysis errors, *i.e.* the analyses are too wet. Averaged over the 5-day period, the mean error of OPER'99 is larger than of MAP-RA at Milano, 2.8 versus 1.7 kg/m^2, respectively.

The comparison of the IWV spatial distribution on 21 Oct 12 UTC indicates the quality of the MAP-RA. High values of IWV prevailing throughout the Po valley (Fig. 23a) are realistically represented in MAP-RA (Fig. 23b), whereas the IWV maxima in CNTRL and particularly in OPER'99 are located at the Ligurian Coast (Fig. 23c,d). The reanalyzed IWV content matches qualitatively as well as quantitatively with GPS derived values, attaining the maxima of more than 32 kg/m^2 close to Venezia and minima across the central Alps with values of less than 12 kg/m^2.

8 Conclusions

The MAP Re-Analysis constitutes an unprecedented description of the state of the atmosphere for the ten-week period in autumn 1999, when the SOP took place in the European Alps. The MAP Re-Analysis has been performed by the global assimilation system 4D-Var at the resolution T511/159L60 which allows a better use of MAP observations over the Alpine region. For instance, 3 times more humidity observations from radiosondes and even 5 times more humidity measurements at surface stations have been assimilated in the Alpine region compared to the operational analysis in 1999.

The main objectives of the MAP Re-Analysis, outlined in the introduction, are being met:

- A comprehensive set of analyses describing the state of the atmosphere for the 70-day period of MAP SOP in autumn 1999 has been produced.
- A formatted archive of the additional MAP observations has been created using BUFR format and has been transfered to the MAP Data Centre (MDC).
- These uniformly formatted MAP observations as well as analyzed fields have been archived at the easily accessible MDC to promote European and international research.
- Validation and diagnostic studies have been performed to understand the impact of the great variety of asynoptic MAP observations and also special care has been devoted to the evaluation of different synoptic features during some Intensive Observation Periods.

Special attention has been paid to European windprofilers, a data source which was not used during the SOP in NWP and only recently has been assimilated at ECMWF. Four of the 16 European windprofilers reporting during the SOP had to be denied in MAP-RA due to their large STD of background departures. These excluded stations comprise two British (Camborne, Dunkeswell), one French (Clermont) and one Italian windprofiler (L'Aquila). The remaining windprofilers have been seen to slightly dry the troposphere in the southern Alpine region and to moisten southern Italy and the Adriatic Sea. The windprofiler data introduce changes in the divergent wind field which feeds back on the humidity analysis.

A twin re-analysis experiment has been accomplished without the use of the MAP observations. When MAP observations are assimilated, the reanalysed fields show slightly moister conditions in the southern Alpine region, southern France and over the Adriatic Sea.

The comparison between the time-series of observed daily precipitation, averaged over the Po catchment south of the Alps, and the forecast daily rainfall (based on the MAP-RA) highlights some aspects of the model skill. The timing and the averaged precipitation amounts agree remarkably well. Furthermore, investigations on IOP2a, IOP2b, IOP8 and IOP15 illustrate some specific aspects of the MAP-RA. Different precipitation patterns in the southern Alpine region, fingerprints of different flow regimes prevailing during IOP2b and IOP8, are well captured by the model. In particular, windprofilers reinforce features as shear zones and jet-stream winds. Also these observations are able to modify the divergent wind field that sometimes has an errorneous feed back in the analyzed humidity. In fact, for IOP2a the increased subsidence (due to Lonate windprofiler) led to a drier boundary layer and consequently inhibits the formation of convection.

Finally, the comparison of GPS derived integrated water vapour contents and the analyzed counterparts shows that the analyses follow the general trend of inter-diurnal humidity variations at southern Alpine GPS stations for two heavy precipitation events (IOP2 and IOP8). Generally, the ECMWF analyses seem to be roughly 2-7 kg/m^2 too dry compared with GPS derived IWV content and they have large spatial and temporal variations. This underestimation of humidity can be partly attributed to the model resolution which plays a crucial role in representing orography and land-sea contrast realistically, both having a strong impact on humidity fields. The dry bias of the Vaisala radiosondes might be another element of explanation.

The timely production of the deliverables and their storage at the public accessible MAP Data Centre will hopefully trigger further research dealing with the MAP SOP and eventually improve our understanding and the prediction of mountain-related atmospheric phenomena.

A Observation errors

Over the years, corrections on observational errors have been derived by statistical evaluation of the performance of the observing system, as component of the assimilation system. The observational errors for wind components, height, temperature and relative humidity are defined at the standard pressure levels. Some RMS (Root Mean Square) values of observation errors relevant for the present investigation are summarized in Table A.1.

Table A.1: Overview of the RMS observation errors of observation types deployed during the MAP campaign.

Observation type	Measured Parameter	3 selected levels		
		1000 hPa	500 hPa	200 hPa
TEMP & PILOT	wind	2.3 m/s	3.0 m/s	3.5 m/s
Windprofiler	wind	2.3 m/s	3.0 m/s	3.5 m/s
TEMP	temperature	1.7 K	1.2 K	1.5 K
TEMP	height	4.3 m	8.4 m	13.2 m
TEMP	relative humidity	0.17	0.17	0.17
SYNOP	relative humidity	0.13		

B Quality assessment of European windprofilers

In order to be able to identify the European windprofilers reporting poor quality measurements, observation statistics has been individually calculated. Generally, the amount and the quality of data is varying significantly among different windprofilers (Fig. B.1). While the Aberystwyth windprofiler is the most active, reporting data from the boundary layer (850 hPa) up to the lower stratosphere (50 hPa), other windprofilers measure only the lower and mid-troposphere (1000 to 700 hPa; e.g. Vienna, Bad Ragaz). Good quality data are reported from the three windprofilers at Aberystwyth (UK), La Ferte Vidame (F) and Lindenberg (D), for which the bias of the background departure is less than 2 m/s in the entire troposphere. However, the bias of some profilers is exceeding values of 4 m/s (3.5 m/s is the observation error in the upper troposphere). Consequently, it has been decided to exclude four of the 16 European windprofilers in the MAP-RA: Camborne (UK), Dunkeswell (UK), Clermont (F) and L'Aquila (I) (Fig. B.1 b,c,h and m).

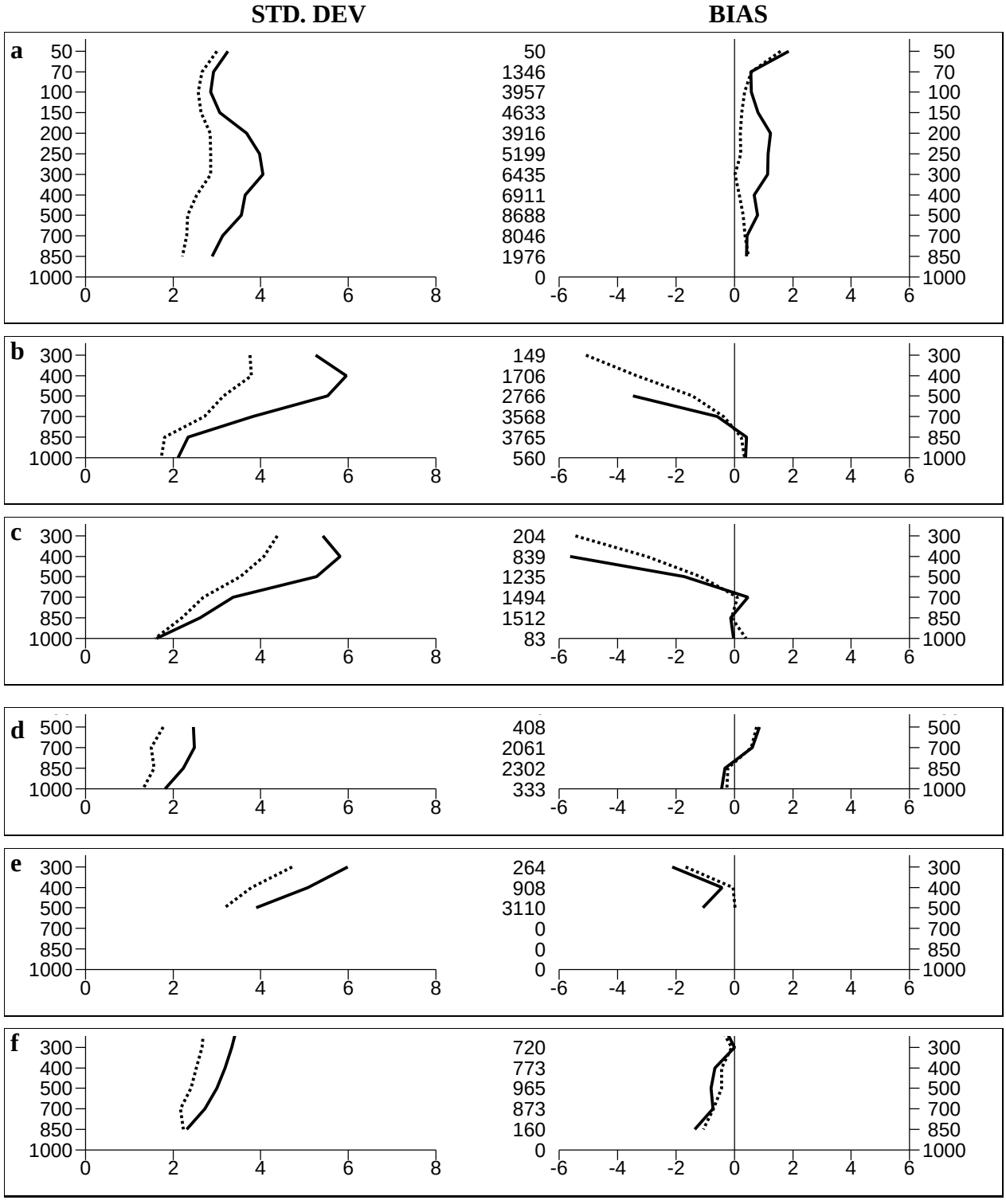

Figure B.1: Standard deviation (left) and bias (right) of the background (o-b; solid line) and analysis (o-a; dotted) departures of the European windprofilers of ALDAT from 7 Sept till 21 Sept 99 : (a) Aberystwyth, (b) Camborne, (c) Dunkeswell, (d) Cabauw, (e) Julier Pass, (f) La Ferte Vidame.

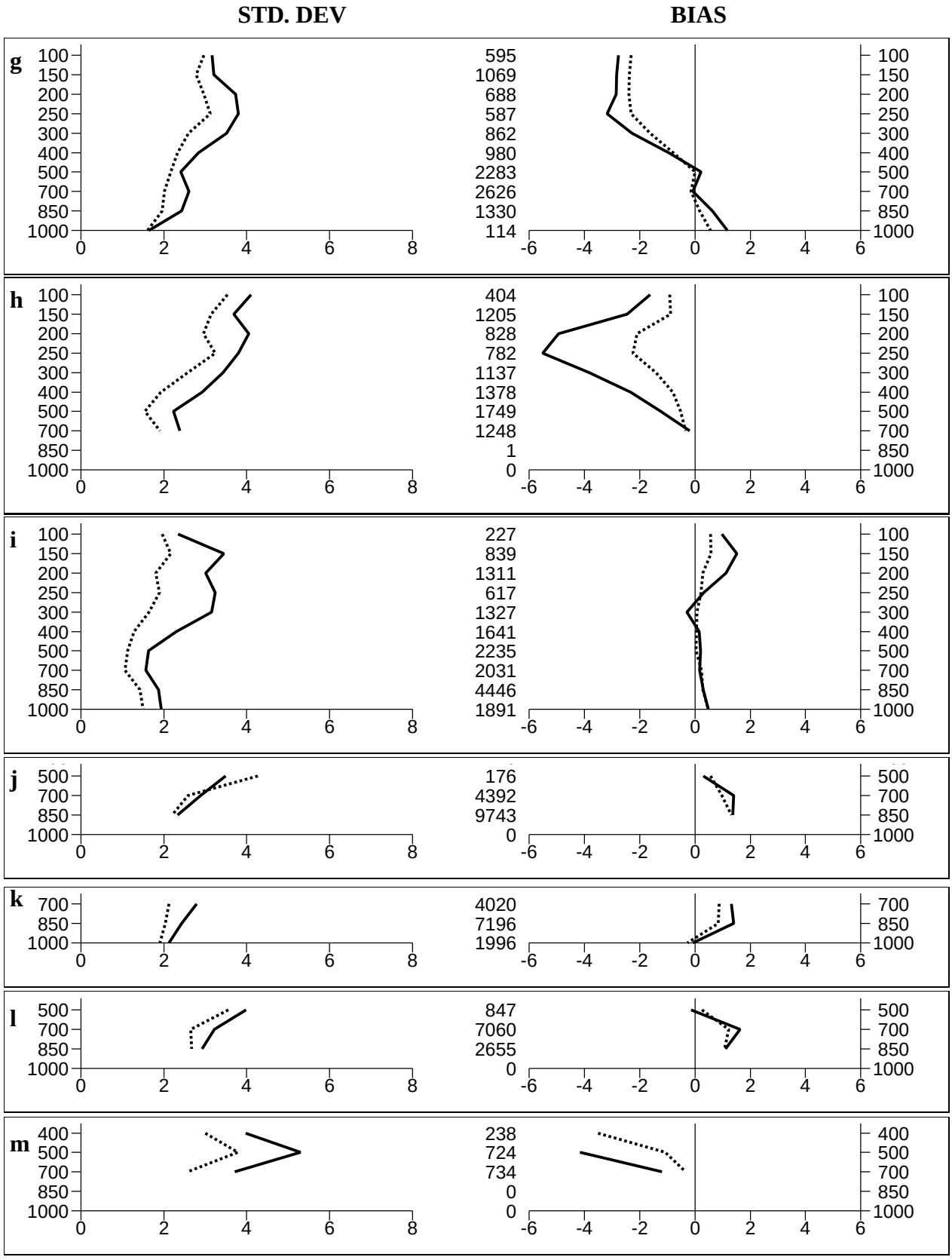

Figure B.1(cont'd): Standard deviation (left) and bias (right) of the background (o-b; solid line) and analysis (o-a; dotted) departures of the European windprofilers: (g) Lonate, (h) Clermont, (i) Lindenberg, (j) Bad Ragaz, (k) Vienna, (l) Innsbruck and (m) L'Aquila.

C Products

C.1 MAP observations

The supplementary observations available for the MAP Re-Analysis project comprise data recorded by roughly 11.000 additional surface stations, an enhanced radiosonde network with some stations reporting every three hours, more than a dozen European windprofilers as well as flight data from 8 research aircrafts from which dropsondes were also released. After the acquisition of these observations from the MAP Data Centre (MDC) in Zürich, the data has been formatted in BUFR code (Tab. C.2). Subsequently, all the observations were archived in 6-hourly intervals and were transfered back to the MDC.

Table C.2: List of MAP observations which have been formatted in BUFR code.

Observing System	BUFR observation	
	type	subtype
Surface stations	0	1
European windprofiler	2	96
Radiosondes	2	101
Dropsondes	2	103
Aircraft data	4	144

C.2 Analyzed fields

The basic analyzed variables include not only the conventional meteorological wind, temperature and humidity fields, but also model products currently available in the ERA-40 Re-Analysis.

The parameters of the MAP Re-Analysis have been archived with a horizontal resolution of T511 for upper air fields, and a reduced Gaussian Grid with approximately uniform 40 km spacing for surface und other grid-point fields. Upper air data (see Table C.3) have been saved at each of the 60 ”full” model levels and at 23 pressure levels. Additionally, a subset of upper air parameters were archived on fifteen isentropic surfaces as well as on the $PV = \pm 2$ surface (for details see ERA-40 Archive Plan, 2000). Surface and single level parameters produced by the analysis are given in Table C.6.

Extra fields from the physical parameterisations accumulated over three hour intervals are post-processed for 12 hour forecasts both at 00 and 12 UTC. The parameters used to validate clear sky radiation, to support trajectory studies and to investigate the net tendencies from parameterised processes, are listed in Tables C.4 and C.5.

Table C.3: Upper air parameters on model (ml) and pressure levels (pl) analyzed three hourly.

Parameter	ml	pl	Code	Units
surface geopotential	x		129	m^2s^{-2}
geopotential		x	129	m^2s^{-2}
temperature	x	x	130	K
specific humidity	x	x	133	$kg\ kg^{-1}$
vertical velocity	x	x	135	$Pa\ s^{-1}$
vorticity	x	x	138	s^{-1}
log surface pressure	x		152	Pa
divergence	x	x	155	s^{-1}
relative humidity		x	157	%
cloud liquid water cont.	x		246	$kg\ kg^{-1}$
cloud ice water cont.	x		247	$kg\ kg^{-1}$
cloud cover	x		248	$(0-1)$

Table C.4: Extra fields accumulated from the physical parameterisations archived at full model levels.

Parameter	Code	Units
Short wave radiative tendency	100	K
Long wave radiative tendency	101	K
Clear sky short wave rad. tendency	102	K
Clear sky long wave rad. tendency	103	K
u tendency	112	ms^{-1}
v tendency	113	ms^{-1}
T tendency	110	K
q tendency	111	kg/kg

Table C.5: Extra fields accumulated from the physical parameterisations saved at half model levels.

Parameter	Code	Units
Updraught mass flux	104	$kg\ m^{-2}$
Downdraught mass flux	105	$kg\ m^{-2}$
Updraught detrainment rate	106	$kg\ m^{-2}$
Downdraught detrainment rate	107	$kg\ m^{-2}$
Total precipitation profile	108	$kg\ m^{-2}$
Turbulent diff. coefficient for heat	109	m^2

Table C.6: Surface and single level parameters analyzed three hourly (as type 4V).

Parameter	Code	Units
sea surface temperature	34	K
sea ice fraction	31	$(0-1)$
surface geopotential	129	m^2s^{-2}
total column water	136	$kg\ m^{-2}$
total column water vapour	137	$kg\ m^{-2}$
soil temperature level 1	139	K
soil temperature level 2	170	K
soil temperature level 3	183	K
soil temperature level 4	236	K
soil moisture (4 levels)	39-42	m^3m^{-3}
Charnock parameter	148	
mean sea level pressure	151	Pa
stand. deviation orography	160	m
anisotropy of orography	161	m
angle of subgrid-scale oro.	162	m
slope of subgrid-scale oro.	163	m
total cloud cover	164	$(0-1)$
10 m eastward wind comp.	165	ms^{-1}
10 m northward wind comp.	166	ms^{-1}
2 metre temperature	167	K
2 metre dewpoint	168	K
downw. surface solar rad.(acc)	169	$Wm^{-2}s$
land/sea mask	172	$(0,1)$
surface roughness	173	m
albedo (climate)	174	
downw. surface thermal rad. (acc)	175	$Wm^{-2}s$
low cloud cover	186	$(0-1)$
medium cloud cover	187	$(0-1)$
high cloud cover	188	$(0-1)$
latitudinal component of gravity wave stress (accum.)	195	$Nm^{-2}s$
meridional component of gravity wave stress (accum.)	196	$Nm^{-2}s$
gravity wave dissipation	197	$Wm^{-2}s$
skin reservoir content	198	m of water
runoff (accum.)	205	m of water
log. surface roughness length (m) for heat	234	
skin temperature	235	K
low vegetation cover	27	$(0-1)$
high vegetation cover	28	$(0-1)$
low vegetation type	29	*index*
high vegetation type	30	*index*
snow temperature	238	K
snow albedo	32	
snow density	33	
snow evaporation (accum.)	44	m
snow melt (accum.)	45	m
sea ice temperature (4 layers)	35-38	K

D MARS retrieval template

The following template is retrieving 3-hourly model level fields of main meteorological parameters T, W, U, V, LNSP, Z and Q for an European area on 17 Sept 1999:

$$
\begin{aligned}
&retrieve,\\
&\quad type &&= 4v,\\
&\quad class &&= rd,\\
&\quad expver &&= e9mi,\\
&\quad stream &&= oper,\\
&\quad AREA &&= 80/-60/20/80,\\
&\quad GRID &&= 256,\\
&\quad DATE &&= 19990917,\\
&\quad TIME &&= 03/15,\\
&\quad STEP &&= 0/3/6/9,\\
&\quad PARAM &&= T/W/U/V/LNSP/Z,\\
&\quad LEVELLIST &&= 1/to/60,\\
&\quad LEVTYPE &&= ML,\\
&\quad REPRES &&= SH,\\
&\quad target &&= 'ml\_4v'\\
&retrieve,\\
&\quad PARAM &&= Q,\\
&\quad REPRES &&= GG,\\
&\quad target &&= 'ml\_4v'
\end{aligned}
$$

Note on type 4*v* and *an*:

The final 4D-Var trajectory is post-processed every 3 hours. Fields called 4v are created with initial date and time the start of the window (03UTC or 15UTC) and steps every 3 hours. The 4v field valid at 12 UTC or 00 UTC, is then renamed as the final analysis (type=an) for the atmospheric fields. The cycling from one cycle to the next is performed by taking these analysis fields, together with the surface fields updated by the SST, snow and soil moisture analyses as input to a 12-hour forecast which produces the background for the next cycle.

Acknowledgments

The MAP Re-Analysis Project was founded by the Mesoscale Alpine Programme of National Weather Services. Thanks to many colleagues at the Centre for helping to perform the Re-Analysis Project at ECMWF. We are grateful to Jan Haseler for the technical support creating the MAP-suite and Milan Dragosavac for BUFRizing the MAP observations. The authors thank Maria Tomassini (DWD) for providing software to convert GPS measured ZTD in IWV. Olivier Bock (CNRS) kindly provided IWV values of the Milano GPS site. Erik Andersson and Anton Beljaars helped to sharpen the line of argument.

References

Andersson, E. and A. Garcia-Mendez, 2002: Assessment of European wind profiler data, in an NWP context, ECMWF Techn. Memo. 372, 14 pp. Available from ECMWF, Shinfield Park, Reading, RG2 9AX, UK.

Bock, O., C. Flamant, E. Richard and C. Keil, 2003: Validation of Precipitable Water from operational analyses and re-analyses with GPS during MAP IOP2A and IOP8, EGS XXVIII General Assembly, Nice, France.

Bougeault, P., P. Binder, A. Buzzi, R. Houze, J. Kuettner, R. B. Smith, R. Steinacker and H. Volkert, 2001: The MAP Special Observing Period. *Bull. Amer. Soc.*, **82**, 433–462.

Bouttier, F., 2001a: The development of 12-hourly 4D-Var, ECMWF Techn. Memo. 348, Available from ECMWF, Shinfield Park, Reading, RG2 9AX, UK.

Bouttier, F., 2001b: The use of profiler data at ECMWF. *Meteor. Z.*, **10**, 497-510.

Cardinali, C., 1999: An assessment of using dropsonde data in numerical weather prediction, ECMWF Techn. Memo. 291, Available from ECMWF, Shinfield Park, Reading, RG2 9AX, UK.

Cardinali, C., L. Isaksen and E. Andersson, 2002: Use and impact of automated aircraft data in 4D-Var, ECMWF Techn. Memo. 371, 17 pp. Available from ECMWF, Shinfield Park, Reading, RG2 9AX, UK.

Ehret, G., K.P. Hoinka, J. Stein, A. Fix, C. Kiemle and G. Poberaj, 1999: Low stratospheric water vapor measured by an airborne DIAL. *J. Geophys. Res.*, **104** (24D), 31 351-31 359.

ERA-40 Archive Plan, 2000: 34pp., available from ECMWF, Shinfield Park, Reading, RG2 9AX, UK

Fovell, R. G. and Y. Ogura, 1988: Numerical simulation of a midlatitude squall-line in two dimensions, *J. Atmos. Sci.* **45**, 3846-3879.

Frei, C. and E. Häller, 2001: Mesoscale precipitation analysis from MAP SOP rain-gauge data. MAP newsletter, **15**, 257-260.

Frei, C. and C. Schär, 1998: A precipitation climatology of the Alps from high-resolution rain-gauge observations. *Int. J. Climatol.*, **18**, 873-900.

Gregory, D., J.-J. Morcrette, C. Jakob, A. Beljaars and T. Stockdale, 2000: Revision of convection, radiation and cloud schemes in the ECMWF Integrated Forecasting System. *Q. J. R. Meteorol. Soc.*, **126**, 1685-1710.

Matricardi, M., F. Chevallier and S. Tjemkes, 2001: An improved general fast radiative transfer model for the assimilation of radiance observations, ECMWF Techn. Memo. 345, 40 pp. Available from ECMWF, Shinfield Park, Reading, RG2 9AX, UK.

Lascaux, F., E. Richard, C. Keil and O. Bock, 2003: Numerical simulations of the precipitation event observed during the MAP IOP2a: Sensitivity to the initial conditions, ICAM/MAP2003 Proceedings, 4pp.

Medina, S. and R. A. Houze Jr, 2003: Air motions and precipitation growth in Alpine storms. *Q. J. R. Meteorol. Soc.*, **129**, 345-371.

Richard, E., S. Cosma, P. Tabary, J.-P. Pinty and M. Hagen, 2003: High-resolution numerical simulations of the convective system observed in the Lago Maggiore area on 17 September 1999 (MAP IOP 2a). *Q. J. R. Meteorol. Soc.*, **129**, 543-564.

Simmons, A. and T. Hollingsworth, 2002: Some aspects of the improvement in skill of numerical weather prediction. *Q. J. R. Meteorol. Soc.*,**128**, 647-678.

Volkert, H., C. Keil, C. Kiemle, G. Poberaj, J.-P. Chaboureau and E. Richard, 2003: Gravity waves over the eastern Alps: A synopsis of the 25 October 1999 event (IOP 10) combining in situ and remote-sensing measurements with a high-resolution simulation. *Q. J. R. Meteorol. Soc.*, **129**, 777-798.